Passivity-based Trajectory Tracking Control in Frictional Oscillators with Set-valued Friction

Aya Younes, Félix Miranda-Villatoro, Bernard Brogliato

Passivity-based Trajectory Tracking Control in Frictional Oscillators with Set-valued Friction

Aya Younes and Félix Miranda-Villatoro and Bernard Brogliato*

November 29, 2024

Abstract

This article is largely concerned with the trajectory tracking control of frictional oscillators, which are nonsmooth nonlinear dynamical systems. The trajectory tracking problem, which is studied under a passivity-based controller addresses three main cases: the nominal case with known friction coefficient, uncertain friction coefficient, and when the Coulomb friction model is enhanced by including Stribeck effects. Monotonicity (or hypomonotonicity) of the friction model is crucial for the stability analysis of the tracking error. It can be relaxed to hypomonotonicity to handle Stribeck model. The framework of linear complementarity systems is used for the analysis. The case of a two-mass system is tackled as an extension of the standard one-mass oscillator. Theoretical results are supported by numerical simulations.

1 Introduction

Frictional oscillators are low-dimension mechanical systems where friction plays a prominent role due to its nonlinear and nonsmooth effects. They have gained significant attention in the Nonlinear Dynamics scientific community due to their applications in mechanical engineering. One-degree-of-freedom oscillators have been widely studied in the Applied Mathematics and in the Bifurcation and Chaos scientific communities, see, *e.g.*, [43, Chapter 9] [47, 48, 46, 27, 30, 69, 31, 45]. These oscillators may also be linked to a simplified Burridge-Knopoff model in seismology, highlighting their practical applications (see [32]). Many authors studied the behaviour of the stick-slip oscillators with various frictional laws see, *e.g.*, [47, 48, 46, 4, 38, 52, 54, 63, 73, 74]. Stability analysis of periodic solutions for periodically excited frictional oscillator were first presented by [30, 69]. Later studies, see, *e.g.*, [63, 55, 42, 54, 27], further investigated the conditions for the existence and the stability of periodic solutions. Externally excited frictional oscillators, as studied in [73, 74, 4, 38],

*Univ. Grenoble Alpes, INRIA, CNRS, Grenoble INP, LJK, 38000 Grenoble, France.

may exhibit chaotic behaviour. These systems often undergo rich bifurcation behaviour, which is explored in [60, 26, 48, 46, 34, 59, 38, 55, 42]. Stick-slip vibrations, which are self-sustained oscillations induced by dry friction are described in [74, 63, 49]. Various control techniques have been developed for the stability analysis of frictional oscillators, including active feedback control to superimpose frictional force in [36], and other control strategies based on delayed time feedback in [28, 51].

Friction is the main source of difficulty in the analysis of frictional oscillators, making its modeling an important step. Given that there is a plethora of friction models, analysis and control of systems with friction have witnessed a significant research interest over the past thirty years both in Automatic Control and Nonlinear Dynamics. Friction models of interest for control may be classified into static models and dynamic models. Static friction includes set-valued or single-valued models. Set-valued models such as Coulomb's friction with constant coefficient or varying coefficient (*e.g.*, Stribeck [6, 53], Dieterich-Ruina [19, Equation (21)]), allow to correctly handle sticking modes at zero relative tangential velocity and are thus essential in multibody applications, contrarily to regularized models which are mainly applied to planar friction where the signum function is replaced by a saturation, or a sigmoid function. Dynamic models with internal state are numerous (LuGre, Leuven, Dahl, elastoplastic *etc* [53]). Dynamic models are better for modeling micro stick-slip effects, though Coulomb with Stribeck coefficient of friction also provides good results in this respect [53]. However, dynamic models also present severe drawbacks [68]. Coulomb friction (with constant coefficient) has limitations [19], but it can also provide quite good results in many instances, see, *e.g.*, [58]. It is sometimes not easy task to choose between a regularized (around zero tangential velocity) model and the set-valued model, see, *e.g.*, [76]. See [11] for a survey on friction models.

Several strategies have been developed for controlling systems with friction. A common approach in the literature is to use model-based friction compensator in the controller. This compensation method can be implemented through feedback control which is based on the actual system states or through feedforward control which is based on the desired system states, see [5, 9, 71, 57, 10], with applications in robotics [56, 61]. However, since it is challenging to model friction exactly, the compensation approach has drawbacks: overcompensating friction that leads to limit cycles and undercompensating friction that leads to steady state errors, see [64] for the analysis of the compensation methods. An adaptive friction compensation control is implemented without a complete model of friction in [61, 72]. Other non-compensation approaches are proposed in [29, 75], where an impulsive control is designed in [75], which has the drawback of having high frequency system dynamics due to high frequency vibrations.

In this article, the friction is modeled by a set-valued signum function, which represents planar Coulomb's friction with constant normal contact force. This function is quite amenable for complementarity [20, 13], allowing the study of frictional oscillators within the framework of linear complementarity systems. This connection to complementarity systems

motivates us to apply some theoretical results from our previous work on trajectory tracking in linear complementarity systems [77] and providing original extensions in this paper. To the best of our knowledge, trajectory tracking for frictional oscillators was not addressed before. This work introduces a different control design approach by integrating friction in the feedback controller which is applied inside the signum function. The control strategy is not to compensate for friction, but rather to use it in a suitable way.

The main contribution of this article is to tackle the trajectory tracking control problem in frictional oscillators with set-valued friction, considering different cases and challenges. The stability result derived from our previous work in [77] is applied to the nominal case in this article, with a new result concerning the complementarity variables. In the case of uncertainties, the controller design and stability analysis apply the theoretical results in [77]. In addition, this article introduces a new approach for the control design based on passifying the friction model when Stribeck effects are incorporated. The previous control strategy is extended to design a trajectory tracking controller for the center of mass of a frictional oscillator with a two-mass system.

This article is organised as follows: section 2 provides useful notations and definitions; Section 3 introduces the dynamics of the simple frictional oscillator within the framework of linear complementarity systems, it addresses well-posedness issues and the characterization of equilibrium points of the error dynamics. The analysis of the desired trajectories is presented in Section 4, followed by the passivity-based control design and the closed-loop error stability analysis for the known parameters case in Section 5. Section 6 is dedicated to study robustness in the presence parametric uncertainties. Section 7 investigates the stability analysis with the Stribeck friction model. Section 8 is dedicated to the tracking control of a two-mass frictional oscillator. To illustrate theoretical results, numerical simulations are provided throughout the article. Conclusions end the article in Section 9, and several useful tools and results are provided in appendix A through appendix D.

2 Preliminaries

This section introduces the notation and definitions necessary for the analyses made in this article. The elements of a matrix $M \in \mathbb{R}^{n\times m}$ are denoted M_{ij}. $M_{\bullet,j}$ is its jth column, and $M_{i,\bullet}$ is its ith row. A matrix $M \in \mathbb{R}^{n\times n}$, possibly nonsymmetric, is said to be positive definite, $M \succ 0$ (resp. positive semi-definite, $M \succcurlyeq 0$) if $x^\top Mx > 0$ for all $x \neq 0 \in \mathbb{R}^n$ (resp. $x^\top Mx \geq 0$). M is a P-matrix if all its principal minors are positive; a positive definite matrix is a P-matrix. The minimum and the maximum eigenvalues of M are denoted $\lambda_{\min}(M)$ and $\lambda_{\max}(M)$. The maximum singular value of $M \in \mathbb{R}^{n\times m}$ is denoted as $\sigma_{\max}(M)$, $\mathrm{Im}(M)$ denotes its image, and $\mathrm{Ker}(M)$ its null space. The singular values are ordered as $\sigma_{\max}(M) = \sigma_1(M) \geq \sigma_2(M) > \ldots > \sigma_r(M) > 0$, where $r = \mathrm{rank}(M)$. Let $M = M^\top$, its eigenvalues are real and ordered as $\lambda_{\max}(M) = \lambda_1(M) \geq \lambda_2(M) \geq \ldots \geq \lambda_n(M) = \lambda_{\min}(M)$. $M^\dagger$ denotes the Moore-Penrose pseudo-inverse of M. The range of the function $f(\cdot)$ is $\mathrm{Im}(f)$,

its domain is $\mathrm{dom}(f) = \{x \mid f(x) < +\infty\}$. Right and left limits of the function $f(\cdot)$ at t are denoted $f(t^+)$ and $f(t^-)$. Let $S \subseteq \mathbb{R}^m$ be a closed convex set containing 0. Its polar cone $S^\circ = \{x \in \mathbb{R}^m \mid x^\top v \leq 0,\ \forall v \in S\} = -S^\star$ where $S^\star$ is the dual cone. AC stands for absolute continuity. Let us recall some useful definitions [17, 65, 66, 25, 16].

Definition 1 *Let $S \subset \mathbb{R}^n$ be a closed, non-empty and convex set. The normal cone to S at $x \in S$ is given by*

$$\mathcal{N}_S(x) = \left\{g \in \mathbb{R}^n \mid g^\top(z - x) \leq 0,\ \ \forall z \in S\right\}. \tag{1}$$

If $x \notin S$, then $\mathcal{N}_S(x) = \emptyset$.

The domain of a set-valued mapping $T : \mathbb{R}^n \rightrightarrows \mathbb{R}^n$ is $\mathrm{Dom}(T) = \{x \in \mathbb{R}^n \mid T(x) \neq \emptyset\}$.

Definition 2 *A multivalued mapping $T : \mathrm{Dom}(T) \subseteq \mathbb{R}^n \rightrightarrows \mathbb{R}^n$ is monotone if for all $u_1, u_2 \in \mathrm{Dom}(T)$, for all $v_1 \in T(u_1)$, $v_2 \in T(u_2)$*

$$\langle u_1 - u_2, v_1 - v_2\rangle \geq 0.$$

It is hypomonotone if there exists a real $k > 0$ such that: $\langle u_1 - u_2, v_1 - v_2\rangle \geq -k||u_1 - u_2||^2$. It is maximal monotone if its graph cannot be enlarged without destroying monotonicity.

Definition 3 *Let $f : \mathbb{R}^n \to \mathbb{R}$ be a proper continuous convex function. A vector $g \in \mathbb{R}^n$ is called a subgradient of f at a point $\bar{x}$ if, for all $x \in \mathbb{R}^n$: $f(x) \geq f(\bar{x}) + g^\top(x - \bar{x})$. The subdifferential of f is the set of all subgradients and is denoted by $\partial f(\bar{x})$.*

Definition 4 *A linear complementarity system (LCS) with inputs is a nonsmooth nonlinear dynamical system defined as:*

$$\begin{cases} (a) & \dot{x}(t) = Ax(t) + B\lambda(t) + Eu(t) \quad \textit{(dt-almost everywhere)} \\ (b) & 0 \leq \lambda(t) \perp w(t) = Cx(t) + D\lambda(t) + Fu(t) \geq 0 \end{cases} \tag{2}$$

where $x(t) \in \mathbb{R}^n$, $\lambda(t) \in \mathbb{R}^m$ and $w(t) \in \mathbb{R}^m$, for all $t \geq 0$, A, B, C, D, E and F are constant matrices of appropriate dimensions, $u : \mathbb{R}_+ \to \mathbb{R}^p$ is an exogenous signal or a control input. The constraint in (2) (b) is the short form of the following three conditions: i) $\lambda(t) \in \mathbb{R}^m_+$, ii) $w(t) = Cx(t) + D\lambda(t) + Fu(t) \in \mathbb{R}^m_+$, and iii) $\langle \lambda(t), w(t)\rangle = 0$. Such constraints describe a linear complementarity problem (LCP) in λ, denoted LCP$(D, Cx + Fu)$.

The LCP (2) (b) states that for $i = 1, \ldots, k$, either $\lambda_i = 0$ or $w_i = 0$. The set of constraints corresponding to the indices where $w_i = 0$ is the set of active constraints and it varies as the system evolves over time. Thus, the LCS in (2) can transition from one operation mode to

another. A state x^* is an equilibrium point of (2) if and only if there exist λ^* and $w^* \in \mathbb{R}^m$ such that the mixed LCP (MLCP)

$$\begin{cases} 0 = Ax^* + B\lambda^* + Eu(t) \\ 0 \leq \lambda^* \perp w^* = Cx^* + D\lambda^* + Fu(t) \geq 0 \end{cases} \tag{3}$$

holds for all $t \geq 0$. It is noteworthy that $\lambda^\star$ may be time-varying.

State jumps, or discontinuities in the solution $x(\cdot)$ occur in LCS (2) at initial time or at times of discontinuity in $Fu(\cdot)$. The formulation of state jumps is based on dissipation principles and is given in [17, Lemma 2.3], [18, 23, 21, 35]. Let us introduce the jump rule briefly.

Definition 5 *[35, Definitions 6, 7] The set of admissible state jumps for LCS in (2) is defined as:*

$$\mathcal{K} \triangleq \{z \in I\!R^n \mid Cz + Fu(t^+) \in Q_D^\star\} \tag{4}$$

*where $Q_D = \{z \in I\!R^m \mid 0 \leq z \perp Dz \geq 0\}$ and $Q_D^\star$ is its dual cone. If (A, B, C, D) is passive with $P = P^\top \succ 0$ and if $0 \in \mathcal{K}$, then the jumps dissipate energy (*i.e., *$V(x(t^+)) \leq V(x(t^-))$) [35, Lemma 3] and the state jump rule is given by:*

$$x(t^+) = \text{argmin}_{x \in \mathcal{K}} \frac{1}{2}(x - x(t^-))^\top P(x - x(t^-)). \tag{5}$$

Definition 6 *A quadruple (A, B, C, D) is said to be passive, or dissipative with respect to the supply rate $\lambda^\top w$, if there exists a non-negative function $V : I\!R^n \to I\!R_+$, called a storage function, such that for all $t_0 \leq t_1$ and all functions $(\lambda, x, w) \in \mathcal{L}_2([t_0, t_1]; I\!R^m \times I\!R^n \times I\!R^m)$ such that $\dot{x}(t) = Ax(t) + B\lambda(t)$, $w(t) = Cx(t) + D\lambda(t)$, the following inequality holds:*

$$V(x(t_0)) + \int_{t_0}^{t_1} \lambda^\top(t) w(t) dt \geq V(x(t_1)) \tag{6}$$

The inequality (6) is called the dissipation inequality. Equivalently, the following linear matrix inequality LMI

$$\begin{pmatrix} A^\top P + PA & PB - C^\top \\ B^\top P - C & -D - D^\top \end{pmatrix} \preccurlyeq 0 \tag{7}$$

has a solution $P = P^\top \succcurlyeq 0$. Then $V(x) = \frac{1}{2} x^\top P x$. The quadruple (A, B, C, D) is said strictly state passive if the LMI (7) holds with $P = P^\top \succ 0$ and $A^\top P + PA + \epsilon P$ for some constant $\epsilon > 0$. It is said strongly passive if the LMI (7) holds with strict inequality and $P = P^\top \succ 0$.

3 Controlled Frictional Oscillators

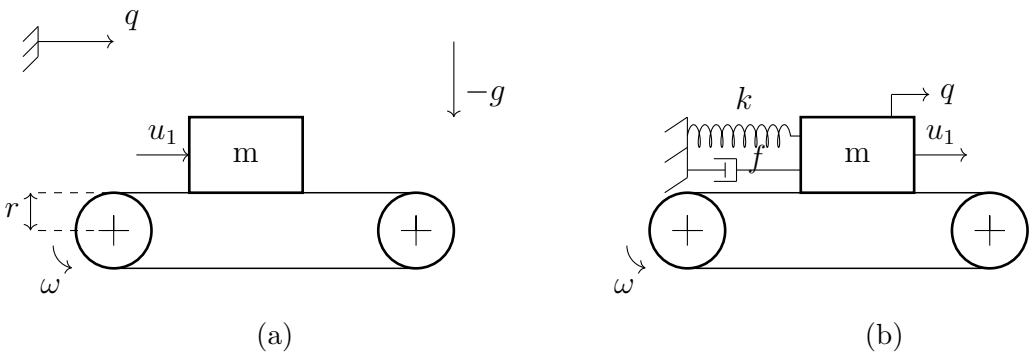

Figure 1: Simple frictional oscillator with Coulomb's friction.

Consider the simple frictional oscillator system depicted in Figure 1a. The objective is to perform trajectory tracking for the mass m, using both the input u_1 and the friction exerted by the belt on the mass (see Remark 1). Assuming that the belt can be given arbitrary velocity, the dynamics of the oscillator are given by:

$$\ddot{q}(t) \in \frac{1}{m}u_1(t) - \mu g \operatorname{sgn}(\dot{q}(t) - u_2(t)) \tag{8}$$

with $u = (u_1, u_2)^\top$, $u_2 = r\omega$ is considered as a control input, $\mu > 0$ is the friction coefficient, ω rad/s is the pulleys' angular velocity, r is their radius, g is the gravity acceleration, m in kg is the mass weigth. Notice that the dynamics (8) can be rewritten as $\ddot{q}(t) = \frac{1}{m}u_1(t) - \mu g \lambda_t(t)$, with $\lambda_t(t) \in \operatorname{sgn}(\dot{q}(t) - u_2(t))$. If $u_1 \equiv 0$ or if $u_1 = u_1(q, \dot{q}, t)$, the dynamics (8) fit within the robot-object class of systems [15] where the robot's dynamics (the pulley-belt system) is neglected: the mass m is the object which can be controlled only through the contact force multiplier $\lambda_t(\cdot)$. Neglecting the friction effects on the belt dynamics so that the pulleys-belt's velocity can be considered not influenced by the friction with the mass, is a common assumption in the Nonlinear Dynamics literature [47, 48, 46, 27, 30, 69, 50], see also references therein. In this setting, we may link the mass to a rigid wall with a linear spring-dashpot model as shown in Figure 1b, yielding the dynamics:

$$\ddot{q}(t) \in \frac{1}{m}u_1(t) - \frac{k}{m}(q(t) - l) - \frac{f}{m}\dot{q}(t) - \mu g \operatorname{sgn}(\dot{q}(t) - u_2(t)) \tag{9}$$

where $k > 0$ is the stiffness, $f > 0$ is the viscous friction coefficient, and l is the natural length of the spring. Under these conditions, the analysis made in the sequel shows that u_1 can be chosen as a feedforward controller that depends only on exogenous signals. It is also noteworthy that u_1 could be chosen as the displacement imposed to one tip of the spring, changing $k(q - l)$ to $k(q + u_1 - l)$ in (9). Provided that k is known, this does not modify the analysis made in the next sections.

Remark 1 *In this work, we do not aim to compensate for friction using the control input u_1. Such compensation is achievable with a first-order sliding-mode controller where the friction term $\mu g \lambda_t$ would be considered as a bounded disturbance, and a sliding surface of the form $\sigma = \dot{\tilde{q}} + \alpha \tilde{q}$. Our strategy is based on using both inputs u_1 and u_2, relying on the monotonicity of friction coupled to passivity of a suitable closed-loop operator for stability analysis. Moreover let us recall that the proposed strategy holds with a simple feedforward input $u_1(t)$ when $f > 0$ and $k > 0$. The price to pay is a particular way to define the desired trajectories.*

3.1 The Complementarity System Framework

The dynamics (8) are equivalently rewritten in a complementarity systems framework as:

$$\begin{cases} \dot{x}(t) = \underbrace{\begin{pmatrix} 0 & 1 \\ 0 & 0 \end{pmatrix}}_{\triangleq A} x(t) + \underbrace{\begin{pmatrix} 0 & 0 \\ \frac{1}{m} & 0 \end{pmatrix}}_{\triangleq E} u(t) + \underbrace{\begin{pmatrix} 0 \\ \mu g \end{pmatrix}}_{\triangleq E'} + \underbrace{\begin{pmatrix} 0 & 0 \\ -2\mu g & 0 \end{pmatrix}}_{\triangleq B} \lambda(t) \\ 0 \leq \lambda(t) \perp w(t) = \underbrace{\begin{pmatrix} 0 & 1 \\ 0 & 0 \end{pmatrix}}_{\triangleq F} u(t) + \begin{pmatrix} 0 \\ 1 \end{pmatrix} + \underbrace{\begin{pmatrix} 0 & 1 \\ -1 & 0 \end{pmatrix}}_{\triangleq D} \lambda(t) + \underbrace{\begin{pmatrix} 0 & -1 \\ 0 & 0 \end{pmatrix}}_{\triangleq C} x(t) \geq 0, \end{cases} \tag{10}$$

with $x = (q, \dot{q})^\top$, $\lambda = (\lambda_1, \lambda_2)^\top$, $u = (u_1, u_2)^\top$. The complementarity conditions in (10) stem from the equivalent representation of the set-valued signum function in [20]. It is verified that the quadruple (A, B, C, D) is passive with storage matrix $P = \begin{pmatrix} p_{11} & 0 \\ 0 & \frac{1}{2g} \end{pmatrix}$. There are two peculiarities to system (10): a) $D \not\succcurlyeq 0$ and $D + D^\top = 0$, b) there are constant terms $\begin{pmatrix} 0 \\ 1 \end{pmatrix} \notin \mathrm{Im}(F)$ and $E' = \begin{pmatrix} 0 \\ -\mu g \end{pmatrix} \in \mathrm{Im}(E)$, hence it does not fit with (2). Solutions to (10) are AC under some conditions on the control input, see below. The first step is the computation of fixed points of (10) in closed-loop, in order to determine whether or not a feedback controller of the form:

$$u(x, \lambda, t) = K[x - x_d(t)] + G[\lambda - \lambda_d(t)] + u_d(t). \tag{11}$$

where x_d, λ_d, u_d are defined later, and with feedback gains $K \in I\!R^{2\times 2}$ and $G \in I\!R^{2\times 2}$, is able to modify the set of equilibria. Notice that $\lambda_1 = \frac{\lambda_t + 1}{2}$ where $\mu m g \lambda_t$ is the tangent interaction force between the mass and the belt, *i.e.*, $\lambda_t \in \mathrm{sgn}(\dot{q} - u_2)$. The multiplier λ_2 is a slack variable has no clear mechanical meaning. It is inferred that only λ_1 is available for feedback. Moreover, we avoid the use of λ_1 in u_1, for otherwise the tangential force could be compensated for directly: this is not a desirable control strategy, see Remark 1. *Most importantly, as alluded to above, our analysis applies to the case when the mass is attached to a rigid wall by a linear spring-dashpot system as in Figure 1b, while u_1 is to be interpreted*

as a feedforward controller, that depends only on $x_d(t)$ and $u_d(t)$. In such a setting, the tracking control problem is that of a mass+spring-dashpot system, with feedforward control u_1 and feedback control u_2 through the tangential contact force which is a maximal monotone operator. These observations constrain the input matrix G to satisfy $G = \begin{pmatrix} 0 & 0 \\ g_{21} & 0 \end{pmatrix}$. It is also noticed that a feedback using λ_2 is useless as it is unable to modify the closed-loop matrix D_{cl} to get strong passivity ($\Rightarrow D_{cl} \succ 0$) instead of strict state passivity, because of the structure of F. In general, it is even better to assume $G = 0$. However, the subsequent analysis shows that $g_{21} > 0$ allows to regularize the set-valued friction and to get robustness that is otherwise impossible to obtain. Inserting (11) to (10), with the above restrictions on G, gives the closed-loop system dynamics:

$$\begin{cases} (a)\ \ \dot{x}(t) = \underbrace{\begin{pmatrix} 0 & 1 \\ \frac{k_{11}}{m} & \frac{k_{12}}{m} \end{pmatrix}}_{\triangleq A_{cl}} x(t) + \underbrace{\begin{pmatrix} 0 & 0 \\ -2\mu g & 0 \end{pmatrix}}_{\triangleq B_{cl}} \lambda(t) - \begin{pmatrix} 0 & 0 \\ \frac{k_{11}}{m} & \frac{k_{12}}{m} \end{pmatrix} x_d(t) + \begin{pmatrix} 0 & 0 \\ \frac{1}{m} & 0 \end{pmatrix} u_d(t) + \begin{pmatrix} 0 \\ \mu g \end{pmatrix} \\ (b)\ \ 0 \leq \lambda(t) \perp w(t) = \overbrace{\begin{pmatrix} k_{21} & -1+k_{22} \\ 0 & 0 \end{pmatrix}}^{\triangleq C_{cl}} x(t) + \overbrace{\begin{pmatrix} g_{21} & 1 \\ -1 & 0 \end{pmatrix}}^{\triangleq D_{cl}} \lambda(t) - \begin{pmatrix} k_{21} & k_{22} \\ 0 & 0 \end{pmatrix} x_d(t) \\ \qquad\qquad - \begin{pmatrix} g_{21} & 0 \\ 0 & 0 \end{pmatrix} \lambda_d(t) + \begin{pmatrix} u_{2d}(t) \\ 1 \end{pmatrix} \geq 0 \end{cases} \tag{12}$$

Remark 2 *No physical parameters appear in the complementarity conditions in (10) or (12), because the complementarity merely represents the set-valued signum function. This will have consequences on the robustness analysis (see section 6). Again it is noteworthy that even a feedback from λ_1 cannot guarantee strong passivity of the closed-loop, because at best $D_{cl} \succcurlyeq 0$. One question which arises is how much $g_{21} \neq 0$ can improve the robustness with respect to uncertainties in μ. This issue is tackled in section 6.*

The system which generates the desired trajectories is:

$$\begin{cases} \dot{x}_d(t) = \begin{pmatrix} 0 & 1 \\ 0 & 0 \end{pmatrix} x_d(t) + \begin{pmatrix} 0 & 0 \\ \frac{1}{m} & 0 \end{pmatrix} u_d(t) + \begin{pmatrix} 0 \\ \mu g \end{pmatrix} + \begin{pmatrix} 0 & 0 \\ -2\mu g & 0 \end{pmatrix} \lambda_d(t) \\ 0 \leq \lambda_d(t) \perp w_d(t) = \begin{pmatrix} 0 & 1 \\ 0 & 0 \end{pmatrix} u_d(t) + \begin{pmatrix} 0 \\ 1 \end{pmatrix} + \begin{pmatrix} 0 & 1 \\ -1 & 0 \end{pmatrix} \lambda_d(t) + \begin{pmatrix} 0 & -1 \\ 0 & 0 \end{pmatrix} x_d(t) \geq 0, \end{cases} \tag{13}$$

where $x_d = (q_d, \dot{q}_d)^\top = (x_{1d}, x_{2d})^\top$. This is equivalent to its differential inclusion form:

$$\ddot{q}_d(t) \in \frac{1}{m} u_{1d}(t) - \mu g \lambda_{t,d}(t), \quad \lambda_{t,d}(t) \in \operatorname{sgn}(\dot{q}_d(t) - u_{2d}(t)) \tag{14}$$

This gives rise to the closed-loop error dynamics $e = x - x_d$:

$$\begin{cases} \dot{e}(t) = \left(\begin{pmatrix} 0 & 1 \\ 0 & 0 \end{pmatrix} + \begin{pmatrix} 0 & 0 \\ \frac{1}{m} & 0 \end{pmatrix} K\right) e(t) + \left(\begin{pmatrix} 0 & 0 \\ -2\mu g & 0 \end{pmatrix} + \begin{pmatrix} 0 & 0 \\ \frac{1}{m} & 0 \end{pmatrix} G\right) (\lambda(t) - \lambda_d(t)) \\ 0 \leq \lambda_d(t) \perp w_d(t) = \begin{pmatrix} 0 & 1 \\ 0 & 0 \end{pmatrix} u_d(t) + \begin{pmatrix} 0 \\ 1 \end{pmatrix} + \begin{pmatrix} 0 & 1 \\ -1 & 0 \end{pmatrix} \lambda_d(t) + \begin{pmatrix} 0 & -1 \\ 0 & 0 \end{pmatrix} x_d(t) \geq 0 \\ 0 \leq \lambda(t) \perp w(t) = \left(\begin{pmatrix} 0 & 1 \\ 0 & 0 \end{pmatrix} K + \begin{pmatrix} 0 & -1 \\ 0 & 0 \end{pmatrix}\right) e(t) - \begin{pmatrix} 0 & 1 \\ 0 & 0 \end{pmatrix} G\lambda_d(t) + \begin{pmatrix} 0 \\ 1 \end{pmatrix} \\ \qquad + \left(\begin{pmatrix} 0 & 1 \\ -1 & 0 \end{pmatrix} + \begin{pmatrix} 0 & 1 \\ 0 & 0 \end{pmatrix} G\right) \lambda(t) + \begin{pmatrix} 0 & -1 \\ 0 & 0 \end{pmatrix} x_d(t) + \begin{pmatrix} 0 & 1 \\ 0 & 0 \end{pmatrix} u_d(t) \geq 0, \end{cases} \tag{15}$$

that is:

$$\begin{cases} \dot{e}(t) = \overbrace{\begin{pmatrix} 0 & 1 \\ \frac{k_{11}}{m} & \frac{k_{12}}{m} \end{pmatrix}}^{A_{cl}} e(t) + \overbrace{\begin{pmatrix} 0 & 0 \\ -2\mu g & 0 \end{pmatrix}}^{B_{cl}} (\lambda(t) - \lambda_d(t)) \\ 0 \leq \lambda_d(t) \perp w_d(t) = \begin{pmatrix} 0 & 1 \\ 0 & 0 \end{pmatrix} u_d(t) + \begin{pmatrix} 0 \\ 1 \end{pmatrix} + \begin{pmatrix} 0 & 1 \\ -1 & 0 \end{pmatrix} \lambda_d(t) + \begin{pmatrix} 0 & -1 \\ 0 & 0 \end{pmatrix} x_d(t) \geq 0 \\ 0 \leq \lambda(t) \perp w(t) = \underbrace{\begin{pmatrix} k_{21} & k_{22} - 1 \\ 0 & 0 \end{pmatrix}}_{C_{cl}} e(t) - \begin{pmatrix} g_{21} & 0 \\ 0 & 0 \end{pmatrix} \lambda_d(t) + \begin{pmatrix} 0 \\ 1 \end{pmatrix} + \underbrace{\begin{pmatrix} g_{21} & 1 \\ -1 & 0 \end{pmatrix}}_{D_{cl}} \lambda(t) \\ \qquad + \begin{pmatrix} 0 & -1 \\ 0 & 0 \end{pmatrix} x_d(t) + \begin{pmatrix} 0 & 1 \\ 0 & 0 \end{pmatrix} u_d(t) \geq 0 \end{cases} \tag{16}$$

with $G = \begin{pmatrix} 0 & 0 \\ g_{21} & 0 \end{pmatrix}$. The closed-loop LCP matrix is D_{cl}.

Remark 3 *It is important to note that* $\text{rank}(B) = \text{rank}(B_{cl}) = 1$. *So, the passification conditions on the rank of the input matrix [16, Theorem 3.61] are not met in this context.*

3.2 Well-posedness of the Closed-loop Dynamics

The well-posedness of (12) and (13) has to be guaranteed as a prerequisite to stability analysis. Let us assume the following:

Assumption 1 *The quadruple* $(A_{cl}, B_{cl}, C_{cl}, D_{cl})$ *in* (12) *is strictly state passive.*

This means that there exist gain matrices K and G such that the following nonlinear matrix inequality with unknowns P, K and G:

$$M \triangleq \begin{pmatrix} (A + EK)^\top P + P(A + EK) & P(B + EG) - (C + FK)^\top \\ (B + EG)^\top P - (C + FK) & -(D + FG) - (D + FG)^\top \end{pmatrix} \preccurlyeq \begin{pmatrix} -\epsilon P & 0 \\ 0 & 0 \end{pmatrix}, \tag{17}$$

has a solution $P = P^\top \succ 0$. This implies that $g_{21} \geq 0$. As examples will show, strict state passivity can hold with $g_{21} = 0$ in certain cases, which may be interesting in practice. Let us examine the well-posedness of the closed-loop system in (12) and of the desired dynamics in (13). First, let us verify that no state jump can occur in the closed-loop system. Indeed, let us consider (5), we obtain: $Q_{D_{cl}} = \begin{pmatrix} 0 \\ I\!R_+ \end{pmatrix}$, $Q^\star_{D_{cl}} = \begin{pmatrix} I\!R \\ I\!R_+ \end{pmatrix}$, and $\mathcal{K}_{cl} = I\!R^2$. Thus, $x(t^+) = x(t^-)$ and there is no state jump in (12), even at times where $\lambda_d(\cdot)$ may be discontinuous. Therefore, solutions to (12), if they exist, must be continuous. Let us deal with the well-posedness of (13), equivalently of (14). Assume that $u_d(\cdot)$ is AC, then posing $z = \dot{q}_d - u_{2d}$ it follows that $\dot{z} = \ddot{q}_d - \dot{u}_{2d}$ where $\dot{u}_{2d}$ is the almost-everywhere derivative of u_{2d}. This gives the DI:

$$\dot{z}(t) \in -\dot{u}_{2d}(t) + \frac{u_{1d}(t)}{m} - \mu g \, \mathrm{sgn}(z(t)). \tag{18}$$

Using for instance [7], it is deduced that the DI in (18) has a unique Lipschitz continuous solution on $[0, T)$ for any $T > 0$, for any $z(0) = z_0 \in I\!R$ and any $u_d(\cdot)$ with $\dot{u}_{1d}(\cdot)$ and $\ddot{u}_{2d}(\cdot)$ bounded in the extended (or local) $\mathcal{L}_2$ norm. Thus, $\dot{q}_d(\cdot)$ is AC (Lipschitzness implies AC), $\ddot{q}_d(\cdot)$ is defined almost everywhere, and $q_d(t) = q_d(0) + \int_0^t \dot{q}_d(s)ds$ is continuously differentiable. However, the multiplier $\lambda_d(\cdot)$ can undergo jumps at some junction times. Therefore, the closed-loop plant (12) is an LCS with exogenous signal $F_{cl}(t) \stackrel{\Delta}{=} -\begin{pmatrix} k_{21} & k_{22} \\ 0 & 0 \end{pmatrix} x_d(t) - \begin{pmatrix} g_{21} & 0 \\ 0 & 0 \end{pmatrix} \lambda_d(t) + \begin{pmatrix} u_{2d}(t) \\ 1 \end{pmatrix}$ entering the complementarity constraints, where no state jump can occur.

Remark 4 *Let us consider the DI in (8). There is in principle no problem in introducing a kind of contact force feedback inside the signum set-valued function. Let $u_2 = u_2(q, \dot{q}, \lambda_t)$, then $\lambda_t \in \mathrm{sgn}(\dot{q} - u_2(q, \dot{q}, \lambda_t)) \Leftrightarrow \dot{q} - u_2(q, \dot{q}, \lambda_t) \in \mathcal{N}_{[-1,1]}(\lambda_t)$, where the inversion of maximal monotone set-valued mapping is used. This is a generalized equation with unknown λ_t, whose well-posedness can be characterized. Indeed, $u_2(q, \dot{q}, \lambda_t) = k_{21}(q - q_d) + k_{22}(\dot{q} - \dot{q}_d) + g_{21}(\lambda_1 - \lambda_{1d}) + u_{2d}$, with $\lambda_1(q, \dot{q}) = \frac{\lambda_t(q,\dot{q})+1}{2}$. This yields when $g_{21} > 0$:*

$$\begin{array}{c} -\dot{q} + k_{21}(q - q_d) + k_{22}(\dot{q} - \dot{q}_d) + g_{21}(\frac{\lambda_t+1}{2} - \lambda_{1d}) + u_{2d} \in -\mathcal{N}_{[-1,1]}(\lambda_t) \\ \Updownarrow \\ \lambda_t(q, \dot{q}) = \mathrm{proj}\left([-1, 1];\ 2\frac{\dot{q} - k_{21}(q-q_d) - k_{22}(\dot{q}-\dot{q}_d) + g_{21}\lambda_{1d} - \frac{g_{21}}{2} - u_{2d}}{g_{21}}\right), \end{array} \tag{19}$$

see Fact A.2. Therefore, the force feedback regularizes the set-valued signum function, as is known in other contexts [13, Remark 2.8] [41]. It is also possible to prove that the LCP in (12) (b) has a unique solution $\lambda(t)$ for any $C_{cl}x(t) + F_{cl}(t)$ and $g_{21} > 0$. In spite of the fact that $D_{cl} \not\succcurlyeq 0$, the result holds due to the special structure of the LCP (especially the second line) and $\mathrm{rank}(D_{cl}) = 2$. Also, the result concerns only $\lambda_1 = \frac{\lambda_t+1}{2}$, not λ_2. It is noteworthy that the multiplier λ_t in (19) depends only on known control parameters, mass

state, and desired signals. This is expected since the LCP in (12) does not involve mechanical parameters. Taking $g_{21} > 0$ means that the multiplier λ_1, solution to the LCP in (12) (b), can be explicitly calculated. So there is no need for a contact force measurement in this case, measurement of x is sufficient to solve the LCP in (12) (b). Note that λ_1 does not depend on μ nor on the normal contact force.

Let us continue the well-posedness study. When $g_{21} = 0$, it follows from [22, Theorems 11 and 26] that the closed-loop system (12) has unique AC solutions. This can be shown using passivity of the quadruple $(A_{cl}, B_{cl}, C_{cl}, D_{cl})$ in Assumption 1, the fact that $\mathrm{Im}(D_{cl} + \mathcal{N}_{\mathbb{R}^2_+}) - F_{cl}(t)) = \mathrm{Im}(D_{cl}) + \mathbb{R}^2_- - F_{cl}(t) = \mathbb{R}^2$ (here a result from [62] is used with the fact that $\mathcal{N}_{\mathbb{R}^2_+}(\cdot) = \mathcal{N}^{-1}_{\mathbb{R}^2_-}(\cdot)$). This together with the fact that $F_{cl}(\cdot)$ is AC allows us to guarantee that [22, Theorem 26 (ii)] holds true. When $g_{21} > 0$ (which will be imposed in some cases), then it follows from (19) that $\lambda_1(\cdot)$ (which is the only component of $\lambda(\cdot)$ that intervenes in (12) (a)) is a Lipschitz continuous function of the state and exogenous terms. Therefore (12) (a) boils down to an ordinary differential equation with Lipschitz continuous right-hand side, existence and uniqueness of locally AC solutions follows from general results [70, Proposition C. 3.8].

The conclusion of this section is that imposing mild conditions on $u_d(\cdot)$ together with passivity as in Assumption 1, guarantees the well-posedness of the closed-loop, the desired, and the error dynamics, with AC states $x(\cdot)$ and $x_d(\cdot)$ (hence the error dynamics (16) is well-posed also).

3.3 Equilibrium Points of the Error System

Let us assume that Assumption 1 holds. As pointed out above this implies that $g_{21} \geq 0$. The equilibria of the LCS (15) are characterized as follows:

Proposition 1 *Consider the error dynamics in (15) or (16). Assume that the quadruple $(A_{cl}, B_{cl}, C_{cl}, D_{cl})$ is strictly state passive. Then, the unique equilibrium point is $e^\star = (0, 0)^\top$ and the multipliers at equilibrium are time-varying such that $\lambda^\star(t) = (\lambda_{1d}(t), |x_{2d}(t) - u_{2d}(t)|)^\top$.*

The proof is in appendix D.

4 Analysis of the Desired Trajectories

This section focuses on the analysis of the desired trajectories generated by the LCS in (13).

4.1 Periodic Trajectories in Frictional Oscillators: a Short Review

In practice, it is certainly interesting to understand which desired trajectories can be designed, in spite of the fact that this is not the main topic of this article. Results on the

construction of periodic solutions of such systems exist in the literature. The physical system considered in [30, 69, 27] is a simple mass-spring dashpot system with dry friction which is different from the system considered in Figure 1a. When addressing the non-sticking behaviour, the solution relies on solving a second-order differential equation which represents the equation of motion. Denhartog [30] provided an exact symmetric and periodic solution for non-sticking motion with $\mu = 1$. His approach starts by assuming that the external force exerted has the form of $F_{ext} = Pcos(\omega t + \phi)$ and that the solution is symmetric (*i.e.,* the period T is divided into two equal half cycles each of length π/ω). The boundary conditions of the steady-state solution were established as follows:

$$\begin{cases} t = 0, \quad x(0) = x_0, \quad \dot{x}(0) = 0 \\ t = \frac{\pi}{\omega}, \quad x(\frac{\pi}{\omega}) = -x_0, \quad \dot{x}(\frac{\pi}{\omega}) = 0 \end{cases} \tag{20}$$

Shaw [69] extended this work to the case where $\mu \neq 1$. He followed the same boundary conditions in (20) for non-sticking motion, then analyzed the stability of the periodic motion. By following the same approach as before (*i.e.,* two turnarounds per cycle and boundary conditions in (20)), the authors in [27] prove mathematically that the $\frac{2\pi}{\omega}$- periodic solutions, where ω is the excitation frequency, are symmetric. This property was previously assumed but not proven yet. Following up from the system studied in [69, 30, 27] where there is no moving belt (*i.e.,* $u_2 = 0$ hence $u_{2d} = 0$), the analysis of the stick/slip behaviour of these trajectories based on the desired input $u_{1d}(t)$ (*i.e.*,the external force applied on the mass m) is illustrated in appendix C.

Let us consider the case when $u_{2d} \neq 0$ which is studied in [47, 48, 46, 4] when u_{2d} is constant and [54] when $u_{2d}(t)$ is time-varying. The stick-slip mechanical system considered in [47, 48, 46] is a simple mass-spring system on a moving belt with constant speed. However, the system presented in Figure 1a differs because it includes an external force $u_{1d}(t)$ acting on the mass and allows for time-varying belt speed $u_{2d}(t)$. In [47], the authors introduce the shooting method as a periodic-solution-finder to address the computational challenges of solving stiff differential equations. To tackle this issue, the authors present the switch model as an alternate friction model to simulate stick-slip vibrations by solving a set of non-stiff differential equations. Furthermore, a time-dependent friction model is studied. The authors in [46] study bifurcations of periodic solutions in mechanical systems with dry friction and discuss the existence of infinitely unstable periodic solutions through repulsion sliding mode in stick/slip mechanical systems.

The paper [37] proposes two numerical methods for the computation of periodic solutions in dynamical systems with maximal monotone right-hand side, including LCS and systems with dry friction. It provides formal justifications to ensure the consistency of the proposed numerical schemes. The results in [37] could be applied to the frictional oscillator we work with, which is represented as an LCS in (13) and, equivalently, as a differential inclusion with maximal monotonicity properties in (14). A recent paper [44] introduces a new method for computing periodic solutions of systems with frictional occurrences. The approach for-

mulates all equations, including friction, as equalities and allows for an exact Coulomb's friction law without regularizing the friction force. This equality-based approach is implemented through a highly compact weighted residual formulation and it represents accurately multiple sticking and sliding phases. Given that Coulomb's friction is represented within the complementarity framework in (10), the method developed in [44] is applicable to design periodic desired trajectories. However this is not investigated further in this article.

4.2 Numerical Example of Periodic Desired Trajectory

This simulation involves implementing a suitable desired input u_d and observe the resulting desired trajectory. The simulation is done with the INRIA software package SICONOS[1][2, 3] dedicated to the simulation of this class of nonsmooth systems. In order to design a periodic desired trajectory x_d, the frictional oscillator is excited by periodic desired input $u_d = (u_{1d}, u_{2d})^\top$ where u_{1d} and u_{2d} have the same period T but different amplitudes, as shown in Figure 2. Take $x_d(0) = (1, 0)^\top$ and the time step $h = 0.01$s.

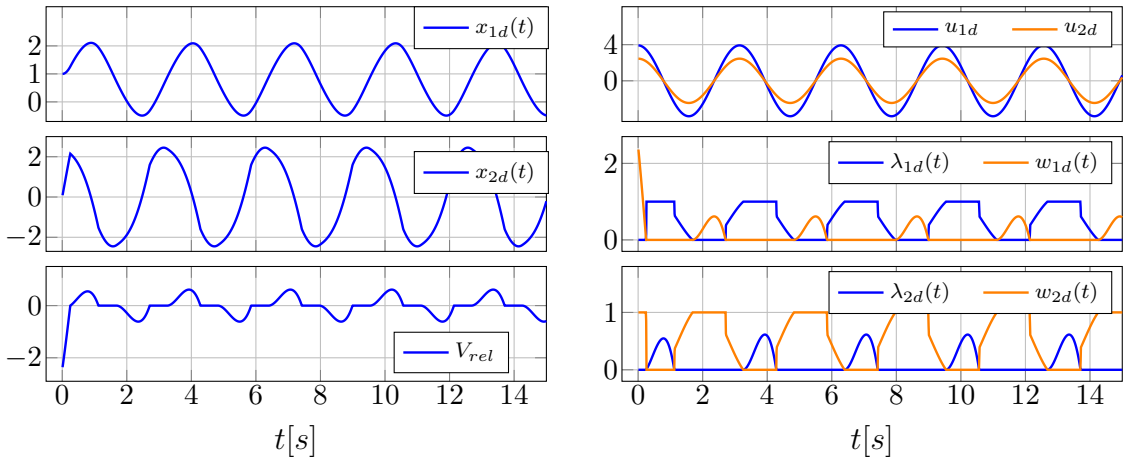

Figure 2: Numerical simulation of (13) with $u_{1d} = 0.8m\mu g \cos 2t$, $u_{2d} = 0.5m\mu g \cos 2t$

The simulation shows a periodic desired trajectory with period $T = \frac{2\pi}{2}$s which is the period of u_d. Interestingly enough the frictional oscillator exhibits both sticking and slipping behaviours, as demonstrated by the relative velocity $V_{rel} = x_{2d} - u_{2d}$ plot.

[1] https://nonsmooth.gricad-pages.univ-grenoble-alpes.fr/siconos/index.html

5 Trajectory Tracking of Frictional Oscillator in Nominal Case

In this section, the trajectory tracking of the frictional oscillator is solved without uncertainties on the friction coefficient. Numerical simulations are presented to illustrate the theoretical result.

5.1 Closed-loop Error Stability Analysis

The stability analysis led in [77], based on the LCS formulations for the nominal case is applied in this section. Assume that all trajectories are AC (see section 3.2). Then, the following results hold. The proof of the first part mimics that of [77, Proposition 3.8] and is recalled for the sake of completeness. The second part is original.

Proposition 2 *Consider the error dynamics (16) with bounded initial conditions, and assume that $(A_{cl}, B_{cl}, C_{cl}, D_{cl})$ is strictly state passive with constant $\epsilon > 0$. Then:* **(i)** *$e(\cdot)$ converges globally exponentially fast to zero;* **(ii)** *When $g_{21} > 0$, the multiplier error $(\lambda_1 - \lambda_{1d})(\cdot)$ converges globally exponentially fast to zero also.*

(i) Consider the Lyapunov candidate function $V(e(t)) = e^\top P e$, with $P = P^\top \succ 0$ the solution of the closed-loop passivity matrix inequality. Then, along the closed-loop error dynamics trajectories:

$$\dot{V}(e(t)) = e^\top (A_{cl}^\top P + P A_{cl}) e(t) + 2e(t)^\top P B_{cl}(\lambda(t) - \lambda_d(t))$$

Starting from (10) and (13), the following is obtained:

$$\begin{cases} w(t) = C_{cl}x(t) + D_{cl}\lambda(t) + Cx_d(t) + Fu_d(t) + \begin{pmatrix} 0 \\ 1 \end{pmatrix} - C_{cl}x_d(t) \\ w_d(t) = C_{cl}x_d(t) + D_{cl}\lambda_d(t) + Cx_d(t) + Fu_d(t) + \begin{pmatrix} 0 \\ 1 \end{pmatrix} - C_{cl}x_d(t). \end{cases}$$

Therefore, it is inferred that:

$$\begin{cases} \lambda(t) \in \mathcal{N}_{S(t)}(C_{cl}x(t) + D_{cl}\lambda(t)) \\ \\ \lambda_d(t) \in \mathcal{N}_{S(t)}(C_{cl}x_d(t) + D_{cl}\lambda_d(t)), \end{cases} \tag{21}$$

with $S(t) \triangleq \{\xi \in I\!R^m \mid \xi + Cx_d(t) + Fu_d(t) + \begin{pmatrix} 0 \\ 1 \end{pmatrix} - C_{cl}x_d(t) \geq 0\}$. From the monotonicity of the normal cone, it follows that:

$$(w(t) - w_d(t))^\top (\lambda(t) - \lambda_d(t)) \leq 0$$

Given that $w(t) - w_d(t) = C_{cl}e(t) + D_{cl}(\lambda(t) - \lambda_d(t))$, $\dot{V}(e(t))$ is written in matrix form as:

$$\begin{aligned}\dot{V}(t) &= \begin{pmatrix} e \\ \Delta\lambda \end{pmatrix}^\top M \begin{pmatrix} e \\ \Delta\lambda \end{pmatrix} + \begin{pmatrix} e \\ \Delta\lambda \end{pmatrix}^\top \begin{pmatrix} 0 & (C+FK)^\top \\ C+FK & D+FG+(D+FG)^\top \end{pmatrix} \begin{pmatrix} e \\ \Delta\lambda \end{pmatrix} \\ &= \begin{pmatrix} e \\ \Delta\lambda \end{pmatrix}^\top M \begin{pmatrix} e \\ \Delta\lambda \end{pmatrix} + 2\Delta\lambda^\top \Delta w \leq \begin{pmatrix} e \\ \Delta\lambda \end{pmatrix}^\top M \begin{pmatrix} e \\ \Delta\lambda \end{pmatrix} \leq -\epsilon\, e(t)^\top P e(t),\end{aligned}$$

where M is the matrix defined in (17) and satisfying the strict state passivity LMI. Hence, $e^\star = 0$ is globally exponentially stable. **(ii)** This follows from the projection form of λ_t in (19) which can be represented as:

$$\lambda_t(q,\dot{q}) = \text{proj}\left([-1,1];\ \frac{2}{g_{21}}\left((\dot{q}-\dot{q}_d) - k_{21}(q-q_d) - k_{22}(\dot{q}-\dot{q}_d) + g_{21}\lambda_{1d} - \frac{g_{21}}{2} + \dot{q}_d - u_{2d}\right)\right)$$

Similarly, $\lambda_{t,d}$ is written as follows

$$\lambda_{t,d} \in \text{sgn}(\dot{q} - u_{2d}) = \text{sgn}\left(\frac{2}{g_{21}}(\dot{q}_d - u_{2d})\right) \quad \Leftrightarrow \quad \lambda_{t,d} = \text{proj}\left([-1,1]; \frac{2}{g_{21}}(\dot{q}_d - u_{2d}) + \lambda_{t,d}\right)$$

Recall that $x \triangleq (q,\dot{q})^\top$ and $x_d \triangleq (q_d,\dot{q}_d)^\top$. Given that $\lambda_t = 2\lambda_1 - 1$ and $\lambda_{t,d} = 2\lambda_{1,d} - 1$, then:

$$\begin{aligned}|\lambda_1 - \lambda_{1d}| &= \tfrac{1}{2}|\lambda_t - \lambda_{t,d}| \\ &= \tfrac{1}{2}\Big|\text{proj}\left([-1,1]; \tfrac{2}{g_{21}}(-[C_{cl}]_{1,\bullet}e + \lambda_{t,d} + x_{2d} - u_{2d})\right) \\ &\quad -\text{proj}\left([-1,1]; \tfrac{2}{g_{21}}(\lambda_{t,d} + x_{2d} - u_{2d})\right) \\ &\leq \tfrac{1}{g_{21}}\left\|C_{cl}e\right\|,\end{aligned} \tag{22}$$

where we have used the Lipschitz continuity property of the projection operator ([8, Proposition 4.8]) to obtain the last inequality. Hence, $\lim_{t\to\infty}|\lambda_1(t) - \lambda_{1d}(t)| \leq \frac{1}{g_{21}}\lim_{t\to\infty}\|C_{cl}e(t)\| = 0$.

5.2 Numerical Simulations

Take $m = 1$ kg, $g = 9.8m/s^2$, and $\mu = 0.5$. Let us take $G = 0$ and check if there exist K and P such that the closed-loop system's quadruple ($A_{cl} = A + EK, B_{cl} = B, C_{cl} = C + FK, D_{cl} = D$) is strictly state passive, which means equivalently solving the BMI in (17). The BMI is transformed into an LMI (see appendix A.1) and solved using MOSEK 9.3.14 solver [1], giving the solution:

$$K = \begin{pmatrix} -1.49 & -1.17 \\ -5.46 & -12.1 \end{pmatrix} \quad \text{and} \quad P = \begin{pmatrix} 1.34 & 0.557 \\ 0.557 & 1.34 \end{pmatrix}, \tag{23}$$

with $\epsilon = 0.01$. Notice that when $G = 0$ in (11), the passivity LMI implies that $PB_{cl} = C_{cl}^\top$ since $D + D^\top = 0$ when $g_{21} = 0$, which yields $-2p_{12}\mu g = k_{21}$ and $-2p_{22}\mu g = k_{22} - 1 < 0$.

Figure 3 shows the numerical simulation of the error dynamical system in (16) with external input $u = (u_1, u_2)^\top = K(x - x_d) + u_d$. Take $x(0) = (0, -1)^\top$, $x_d(0) = (1, 0)^\top$ and the time step $h = 0.01$.

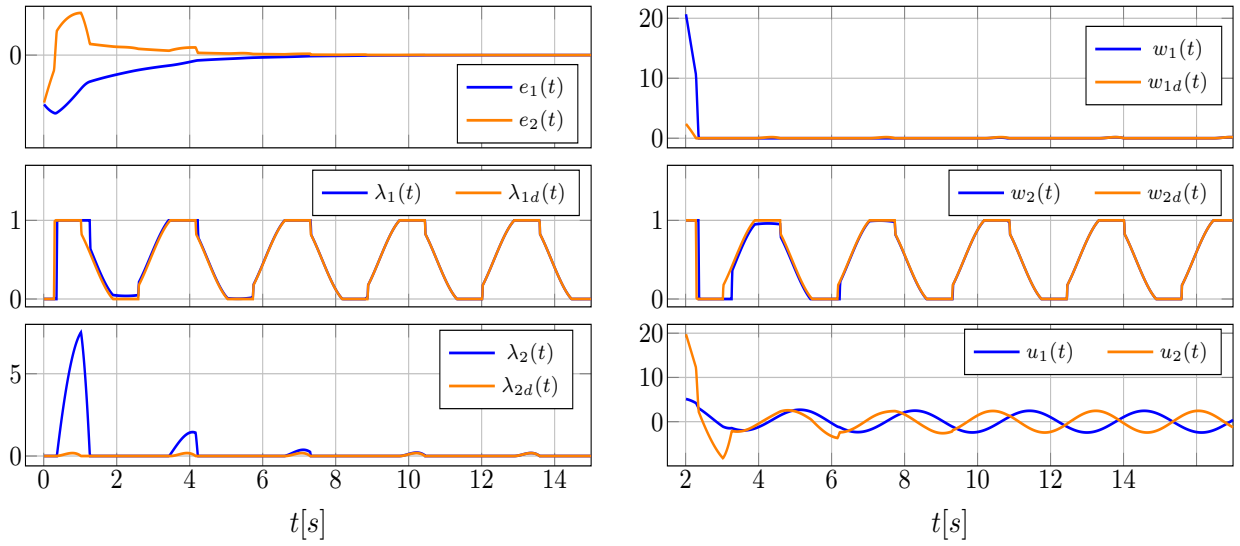

Figure 3: Simulation of the error dynamics (16), with $u_{1d} = u_{2d} = 0.5m\mu g \cos 2t$ and $G = 0$.

The numerical simulation demonstrates that tracking of the desired trajectory x_d is achieved without the requirement of an additional feedback from λ_1 (*i.e.*, $G = 0$). Additionally, it is interesting to observe that the complementarity variables of the closed-loop system (λ and w) converge to the complementarity variables of the desired system (λ_d and w_d). The controller u shows a periodic behaviour in the steady state response (*i.e.*, $e = x - x_d = 0$), where u converges to the periodic desired input u_d.

6 Parametric Robustness Analysis

This section is dedicated to analyse the robustness of the above scheme, which is designed assuming the strict state passivity of the closed-loop system. As shown in [77], strong passivity of $(A_{cl}, B_{cl}, C_{cl} D_{cl})$ in (12) ensures robustness against a large class of uncertainties. However, strong passivity of this quadruple cannot be achieved for (12). The analysis focuses on the case when uncertainties $\Delta\mu$ are present in the friction coefficient μ, which is supposed to be known only with a nominal value $\mu_0 > 0$. Then, it is crucial that the multiplier λ_1 is used in the controller, with $g_{21} > 0$. The analysis in this section relies on theoretical results from [77], specifically Propositions 7, 8 and Lemma 2 which are presented in appendix B.

6.1 Robustness analysis with bounded and time-varying uncertainties $\Delta\mu(\dot{q}_{rel}) = \mu(\dot{q}_{rel}) - \mu_0$

Let us recall that $\dot{q}_{rel} = \dot{q} - u_2$. Here, we consider that the nominal friction coefficient μ_0 (used in the desired dynamics and the nominal model of the plant) and the "real" plant's friction coefficient μ are not the same. It could even be that μ_0 is chosen constant while $\mu = \mu(t, \dot{q})$, then $\Delta\mu(\dot{q}_{rel}) = \mu(\dot{q}_{rel}) - \mu_0$. From (10) the uncertainties satisfy:

$$\Delta A = 0, \Delta C = 0, \Delta D = 0, \Delta E = 0, \Delta F = 0, \Delta B = \begin{pmatrix} 0 & 0 \\ -2g\Delta\mu & 0 \end{pmatrix}, \Delta E' = \begin{pmatrix} 0 \\ g\Delta\mu \end{pmatrix}. \quad (24)$$

Compared to [77], the uncertainties are much simpler to handle. This will allow us to analyse the robustness in detail. The closed-loop system in (12) cannot be made strongly passive (see Remark 2). Thus, it is not possible to apply directly the results of robustness analysis for LCS from [77]. Instead, let us relax the conditions of strong passivity by applying the results derived in [77, section 4.3] (see appendix B) to address the robustness analysis in frictional oscillators. The desired system dynamics in (13) are written as:

$$\begin{cases} \dot{x}_d(t) = A_0 x_d(t) + B_0 \lambda_d(t) + E_0 u_d(t) + E_0' \\ 0 \leq \lambda_d(t) \perp w_d(t) = C_0 x_d(t) + D_0 \lambda_d(t) + F_0 u_d(t) + F_0' \geq 0 \end{cases}$$

where $A_0 = \begin{pmatrix} 0 & 1 \\ 0 & 0 \end{pmatrix}$, $B_0 = \begin{pmatrix} 0 & 0 \\ -2\mu_0 g & 0 \end{pmatrix}$, $C_0 = \begin{pmatrix} 0 & -1 \\ 0 & 0 \end{pmatrix}$, $D_0 = \begin{pmatrix} 0 & 1 \\ -1 & 0 \end{pmatrix}$, $E_0 = \begin{pmatrix} 0 & 0 \\ \frac{1}{m} & 0 \end{pmatrix}$, $F_0 = \begin{pmatrix} 0 & 1 \\ 0 & 0 \end{pmatrix}$, $E_0' = \begin{pmatrix} 0 \\ \mu_0 g \end{pmatrix}$ and $F_0' = \begin{pmatrix} 0 \\ 1 \end{pmatrix}$. The dynamics of the closed-loop system in (12) with parametric uncertainties are written as:

$$\begin{cases} \dot{x}(t) = (A_0 + E_0 K_0)x(t) + (B_0 + \Delta B)\lambda(t) - E_0 K_0 x_d(t) + E_0 u_d(t) + E_0' + \Delta E' \\ 0 \leq \lambda(t) \perp w(t) = (C_0 + F_0 K_0)x(t) + (D_0 + F_0 G_0)\lambda(t) - F_0 K_0 x_d(t) - F_0 G_0 \lambda_d(t) \\ \qquad +F_0 u_d(t) + F_0' \geq 0 \end{cases} \quad (25)$$

where K_0 and G_0 are computed solving the nominal system matrix inequality as in (17), see the proof of Proposition 3. The closed-loop error dynamics ($e = x - x_d$) are:

$$\begin{cases} \dot{e}(t) = A_{cl} e(t) + B_{cl}\Delta\lambda(t) + \Delta B\lambda(t) + \Delta E' \\ \Delta w(t) = w(t) - w_d(t) = C_{cl} e(t) + D_{cl}\Delta\lambda(t) \\ 0 \leq \lambda(t) \perp w(t) \geq 0 \quad \text{and} \quad 0 \leq \lambda_d(t) \perp w_d(t) \geq 0 \end{cases} \quad (26)$$

where $\Delta\lambda(t) = \lambda(t) - \lambda_d(t)$ and $A_{cl} = A_0 + E_0 K_0, B_{cl} = B_0, C_{cl} = C_0 + F_0 K_0$ and $D_{cl} = D_0 + F_0 G_0$. The stability result is stated as follows.

Proposition 3 *Consider the error dynamics in (26). Assume that:*

- *(i) The uncertainties are bounded such that* $\Delta B^\top \hat{\Lambda}_B^{-1} \Delta B \preccurlyeq \begin{pmatrix} 1 & 0 \\ 0 & 0 \end{pmatrix}$ *and* $\Delta E'^\top \hat{\Lambda}_1^{-1} \Delta E' \preccurlyeq I_m$*, given the matrices* $\hat{\Lambda}_k = \hat{\Lambda}_k^\top \succ 0$ *where* $k \in \{1, B\}$*.*
- *(ii) There exists a matrix* $P_0 = P_0^\top \succ 0$ *such that the quadruple* $(A_{cl}, B_0, C_{cl}, D_{cl})$*, corresponding to the nominal closed-loop system in (12) with* $\mu = \mu_0$*, is strictly state passive with* $\epsilon > 0$*.*
- *(iii) The control gain* $G = \begin{pmatrix} 0 & 0 \\ g_{21} & 0 \end{pmatrix}$ *is chosen such that* $g_{21} > \frac{1}{2}$*.*
- *(iv) The following inequality holds:*

$$\sigma_{\max}\left(-P_0(\hat{\Lambda}_1 + \hat{\Lambda}_B)P_0\right) + \sigma_{\max}\left(\left(-P_0 B_0 + C_{cl}^\top\right)\left(-B_0^\top P_0 + C_{cl}\right)\right) \leq \epsilon \lambda_{\max}(P_0)$$

for $P_0 = P_0^\top \succ 0$ *and* $\epsilon > 0$*.*

Then, the solution of the error dynamics in (26) is globally uniformly ultimately bounded (GUUB), satisfying: $\|e\| \leq \sqrt{\frac{\lambda_{\max}(P_0)\lambda_{\min}^{-1}(\hat{\Lambda}_1)\rho}{\lambda_{\min}^2(P_0)\epsilon'}}$*, where* $\rho = \frac{det(\hat{\Lambda}_B)}{\hat{\Lambda}_{B_{11}}}$ *defines the bound on* ΔE*.*

For the sake of notation simplicity, the matrices M_0 and ΔM_0 are not explicitly stated in the theorem. These matrices are defined in the following proof. The proof is divided into two main parts. In the first part, a suitable storage function is derived for the error dynamics in (26) to serve as a Lyapunov function. Then, the second part presents explicit conditions to prove that the Lyapunov function decreases.

Construction of Lyapunov function The storage function $V(t) = e^\top P_0 e$ where P_0 is the solution of the strict state passivity BMI transformed into LMI (see appendix A.1) given by: $M_0 \preccurlyeq \begin{pmatrix} -\epsilon P_0 & 0 \\ 0 & 0 \end{pmatrix}$ where M_0 is defined as:

$$M_0 \triangleq \begin{pmatrix} A_{cl}^\top P_0 + P_0 A_{cl} & P_0 B_{cl} - C_{cl}^\top \\ B_{cl}^\top P_0 - C_{cl} & -D_{cl} - D_{cl}^\top \end{pmatrix} \tag{27}$$

Let us define $p(t, \lambda) \triangleq \Delta B \lambda(t) + \Delta E'$. The rate of change of the storage function is:

$$\dot{V} = e^\top (A_{cl}^\top P_0 + P_0 A_{cl}) e + 2e^\top P_0 B_{cl} \Delta\lambda + 2e^\top P_0 p(t, \lambda) \pm 2\Delta\lambda^\top \Delta w \tag{28}$$

The added and subtracted term is to recover the matrix M_0 in (27). In matrix form, it is represented as:

$$2\Delta\lambda^\top \Delta w = \begin{pmatrix} e \\ \Delta\lambda \end{pmatrix}^\top \begin{pmatrix} 0 & C_{cl}^\top \\ C_{cl} & D_{cl} + D_{cl}^\top \end{pmatrix} \begin{pmatrix} e \\ \Delta\lambda \end{pmatrix}$$

Then,

$$\dot{V} = \begin{pmatrix} e \\ \Delta\lambda \end{pmatrix}^\top M_0 \begin{pmatrix} e \\ \Delta\lambda \end{pmatrix} + 2e^\top P_0 p(t,\lambda) + 2\Delta\lambda^\top \Delta w \tag{29}$$

Let us substitute the expression of $p(t,\lambda)$ in (29), then:

$$\dot{V} = \begin{pmatrix} e \\ \Delta\lambda \end{pmatrix}^\top M_0 \begin{pmatrix} e \\ \Delta\lambda \end{pmatrix} + \begin{pmatrix} e \\ \Delta\lambda \end{pmatrix}^\top \begin{pmatrix} 0 & P_0\Delta B \\ \Delta B^\top P_0 & 0 \end{pmatrix} \begin{pmatrix} e \\ \Delta\lambda \end{pmatrix} + 2e^\top P_0 \Delta E' + 2\Delta\lambda^\top \Delta w$$

By considering monotonicity of the mapping $-\lambda \mapsto w$ (or $-\lambda_d \mapsto w_d$) in (26), the following inequality is obtained:

$$\dot{V} \leq -\begin{pmatrix} e \\ \Delta\lambda \end{pmatrix}^\top (-M_0 + \Delta M_0) \begin{pmatrix} e \\ \Delta\lambda \end{pmatrix} + 2e^\top P_0 \Delta E'$$

with $\Delta M_0 \triangleq \begin{pmatrix} 0 & -P_0\Delta B \\ -\Delta B^\top P_0 & 0 \end{pmatrix}$. For any $\hat{\Lambda}_1^\top = \hat{\Lambda}_1 \succ 0$, the following holds:

$$|2e^\top P_0 \Delta E'| \leq e^\top P_0 \hat{\Lambda}_1 P_0 e + \Delta E'^\top \hat{\Lambda}_1^{-1} \Delta E'$$

Thus,

$$\dot{V} \leq -\begin{pmatrix} e \\ \Delta\lambda \end{pmatrix}^\top \left(-M_0 + \Delta M_0 - \begin{pmatrix} P_0\hat{\Lambda}_1 P_0 & 0 \\ 0 & 0 \end{pmatrix}\right) \begin{pmatrix} e \\ \Delta\lambda \end{pmatrix} + \Delta E'^\top \hat{\Lambda}_1^{-1} \Delta E' \tag{30}$$

The expression $\begin{pmatrix} e \\ \Delta\lambda \end{pmatrix}^\top \Delta M_0 \begin{pmatrix} e \\ \Delta\lambda \end{pmatrix}$ is equivalently written as: $-2e^\top P_0 \Delta B \Delta\lambda$. Take $\hat{\Lambda}_B = \begin{pmatrix} d & e \\ e & f \end{pmatrix} \succ 0$ for some $d, e, f \in \mathbb{R}$. Let us assume that:

$$\Delta B^\top \hat{\Lambda}_B^{-1} \Delta B = \frac{1}{df - e^2} \begin{pmatrix} 4g^2\Delta\mu^2 d & 0 \\ 0 & 0 \end{pmatrix} \preccurlyeq \begin{pmatrix} 1 & 0 \\ 0 & 0 \end{pmatrix} \tag{31}$$

Let $z \triangleq \begin{pmatrix} e \\ \Delta\lambda \end{pmatrix}$, then

$$z^\top \left[-M_0 + \Delta M_0 - \begin{pmatrix} P_0\hat{\Lambda}_1 P_0 & 0 \\ 0 & 0 \end{pmatrix}\right] z \geq z^\top \begin{pmatrix} -(M_0)_{11} - P_0(\hat{\Lambda}_1 + \hat{\Lambda}_B)P_0 & -(M_0)_{12} \\ -(M_0)_{21} & -(M_0)_{22} - \hat{I} \end{pmatrix} z$$

where $\hat{I} \triangleq \begin{pmatrix} 1 & 0 \\ 0 & 0 \end{pmatrix}$. Let us define:

$$\begin{aligned} \hat{L} &\triangleq -M_0 + \Delta M_0 - \begin{pmatrix} P_0\hat{\Lambda}_1 P_0 & 0 \\ 0 & 0 \end{pmatrix} - \begin{pmatrix} \epsilon' P_0 & 0 \\ 0 & 0 \end{pmatrix} \\ &\triangleq \begin{pmatrix} -A_{cl}^\top P_0 - P_0 A_{cl} - P_0(\hat{\Lambda}_1 + \hat{\Lambda}_B)P_0 - \epsilon' P_0 & -P_0 B_{cl} + C_{cl}^\top \\ -B_{cl}^\top P_0 + C_{cl} & D_{cl} + D_{cl}^\top - \hat{I} \end{pmatrix} \succcurlyeq 0 \end{aligned} \tag{32}$$

The term $\epsilon' P_0$ is introduced for bounding the error as will be shown later. For stability analysis, it is required to prove that $\dot{V} \leq 0$ holds in a certain domain to be defined. This means that it is necessary to show that the matrix inequality $\hat{L} \succcurlyeq 0$ holds for $\epsilon' > 0$, as detailed below.

Conditions for $\hat{L} \succcurlyeq 0$ in (32) to hold true The conditions presented below are derived from proving positive semi-definiteness, relaxing strong passivity into strict state passivity (see appendix B). Take

$$\hat{Q} \triangleq \underbrace{-A_{cl}^\top P_0 - P_0 A_{cl} - \epsilon' P_0}_{\hat{Q}_0} + \underbrace{(-P_0(\hat{\Lambda}_1 + \hat{\Lambda}_B)P_0)}_{\Delta\hat{Q}},$$

$\hat{S} \triangleq \underbrace{-P_0 B_{cl} + C_{cl}^\top}_{\hat{S}_0}$ and $\hat{R} \triangleq \underbrace{D_{cl} + D_{cl}^\top}_{\hat{R}_0} + \underbrace{(-\hat{I})}_{\Delta\hat{R}}$, where $P_0 = \begin{pmatrix} p_{11} & p_{12} \\ p_{12} & p_{22} \end{pmatrix}$ such that $P_0 = P_0^\top \succ 0$, is the solution of $M_0 \preccurlyeq \begin{pmatrix} -\epsilon P_0 & 0 \\ 0 & 0 \end{pmatrix}$ with M_0 defined in (27). Recall that $\hat{\Lambda}_1 = \begin{pmatrix} a & b \\ b & c \end{pmatrix} \succ 0$ for some $a, b, c \in I\!R$. The matrices A_{cl}, B_{cl}, C_{cl} and D_{cl} are defined in (12). Let us explicitly write the matrices $\hat{Q} = \hat{Q}_0 + \Delta\hat{Q}$, $\hat{R} = \hat{R}_0 + \Delta\hat{R}$ and $\hat{S} = \hat{S}_0$:

$$\hat{Q}_0 = \begin{pmatrix} -2p_{12}\frac{k_{11}}{m} - \epsilon' p_{11} & -p_{11} - \frac{k_{12}}{m}p_{12} - \frac{k_{11}}{m}p_{22} - \epsilon' p_{12} \\ -p_{11} - \frac{k_{12}}{m}p_{12} - \frac{k_{11}}{m}p_{22} - \epsilon' p_{12} & -2p_{12} - 2\frac{k_{12}}{m}p_{22} - \epsilon' p_{22} \end{pmatrix},$$

$$-\Delta\hat{Q} = \begin{pmatrix} p_{11}^2(a+d) + p_{12}^2(c+f) + 2p_{11}p_{12}(b+e) & (p_{12}^2 + p_{11}p_{22})(b+e) + p_{11}p_{12}(a+d) + p_{12}p_{22}(c+f) \\ (p_{12}^2 + p_{11}p_{22})(b+e) + p_{11}p_{12}(a+d) + p_{12}p_{22}(c+f) & p_{12}^2(a+d) + p_{22}^2(c+f) + 2p_{12}p_{22}(b+e) \end{pmatrix},$$

$$\hat{S} = \hat{S}_0 = \begin{pmatrix} 2p_{12}\mu g + k_{21} & 0 \\ 2p_{22}\mu g - 1 + k_{22} & 0 \end{pmatrix}, \quad \hat{R}_0 = \begin{pmatrix} 2g_{21} & 0 \\ 0 & 0 \end{pmatrix}, \quad \text{and} \quad \Delta\hat{R} = \begin{pmatrix} -1 & 0 \\ 0 & 0 \end{pmatrix},$$

where the constants a, b, c, d, e and f are all defined above. By considering the conditions for positive semi-definiteness in Definition 1, the matrix $\hat{L} \triangleq \begin{pmatrix} \hat{Q}_0 + \Delta\hat{Q} & \hat{S}_0 \\ \hat{S}_0^\top & \hat{R}_0 + \Delta\hat{R} \end{pmatrix} \succcurlyeq 0$ if and only if:

1. $\hat{R} \succcurlyeq 0 \Leftrightarrow \begin{pmatrix} 2g_{21} - 1 & 0 \\ 0 & 0 \end{pmatrix} \succcurlyeq 0$ which is satisfied for all g_{21} such that $g_{21} \geq \frac{1}{2}$.

2. $\mathrm{Im}(\hat{S}^\top) \subseteq \mathrm{Im}(\hat{R})$ and this condition holds as a consequence of the following:

$$\begin{aligned} &\mathrm{Im}(\hat{S}_0^\top) = \mathrm{Im}(\hat{S}^\top) \\ &= \left\{ w \in I\!R^2 \mid w = \begin{pmatrix} (2\mu g p_{12} + k_{12})x + (2\mu g p_{22} - 1 + k_{22})y \\ 0 \end{pmatrix} \text{ for some } x,\ y \in I\!R \right\} \\ &\subseteq \mathrm{Im}(\hat{R}) = \left\{ w \in I\!R^2 \mid w = \begin{pmatrix} (2g_{21} - 1)t \\ 0 \end{pmatrix} \text{ for some } t \in I\!R \right\} \end{aligned}$$

3. $\hat{Q} \succeq \hat{S}\hat{R}^{\dagger}\hat{S}^{\top}$. Let us follow the conditions presented in Proposition 8 in order to check the validity of this item (*i.e.,* $Q \succeq SR^{\dagger}S^{\top}$), then: (i) $\hat{R} \succcurlyeq 0$ for $g_{21} \geq \frac{1}{2}$, (ii) $\text{Im}(\Delta R) = \left\{ w \in I\!R^2 \mid w = \begin{pmatrix} -y \\ 0 \end{pmatrix} \text{for some } y \in I\!R \right\} \subseteq \text{Im}(R_0) = \left\{ w \in I\!R^2 \mid w = \begin{pmatrix} 2g_{21}x \\ 0 \end{pmatrix} \text{for some } x \in I\!R \right\}$ for any $x \in I\!R$, (iii) $\text{rank}(R_0) = 1$, $\sigma_{\max}(\Delta R) = 1 < \sigma_1(R_0) = 2g_{21}$ which holds for $g_{21} > \frac{1}{2}$, (iv) $\sigma_{\max}(OT) + \sigma_{\max}(\Delta\hat{Q}) < \epsilon\lambda_{\max}(P_0)$ where OT is defined in (8) and in this case, where $\Delta\hat{S} = 0$, it is written as:

$$OT = -\hat{S}_0\hat{R}_0^{\dagger}\Delta\hat{R}\hat{R}_0^{\dagger}\hat{S}_0^{\top}$$

with $\hat{R}_0^{\dagger} = \begin{pmatrix} \frac{1}{2g_{21}} & 0 \\ 0 & 0 \end{pmatrix}$. Some manipulations yield:

$$\begin{aligned} OT &= \frac{1}{4g_{21}^2} \begin{pmatrix} (2p_{12}\mu g + k_{21})^2 & (2p_{12}\mu g + k_{21})(2p_{22}\mu g - 1 + k_{22}) \\ (2p_{22}\mu g - 1 + k_{22})(2p_{12}\mu g + k_{21}) & (2p_{22}\mu g - 1 + k_{22})^2 \end{pmatrix} \\ &= \frac{1}{4g_{21}^2}\hat{S}_0\hat{S}_0^{\top} \end{aligned} \tag{33}$$

According to [12, Fact 5.11.5] and given that OT is positive semi-definite, $\sigma_i(OT) = \lambda_i(OT)$ for $i \in 1, 2$. Then, $\sigma_{\max}(OT) = \frac{1}{4g_{21}^2}\left((2p_{12}\mu g + k_{21})^2 + (2p_{22}\mu g - 1 + k_{22})^2\right) > 0$. Given that $P_0 = P_0^{\top} \succ 0$, then $\lambda_{\max}(P_0) > 0$. Note that the matrices $\Delta\hat{Q}$ and $-(\hat{\Lambda}_1 + \hat{\Lambda}_B)$ are congruent, so they have the same number and signs of eigenvalues [39, Theroem 4.5.8]. This means that $\lambda_i(\Delta\hat{Q}) < 0$ for $i \in \{1, 2\}$. Assume that $\hat{\Lambda}_1 = \alpha I_2$ and $\hat{\Lambda}_B = \beta I_2$, $\alpha > 0$, $\beta > 0$, then $\Delta\hat{Q} = -(\alpha+\beta)P_0^2$ which is symmetric (*i.e.,* $\Delta\hat{Q} = \Delta\hat{Q}^{\top}$). As $P_0 = P_0^{\top} \succ 0$, it follows that $\sigma_i(P_0) = \lambda_i(P_0)$. Thus, $\sigma_{\max}(\Delta\hat{Q}) = (\alpha + \beta)\lambda_{\max}^2(P_0)$. Hence, item (iv) is written as: $(\alpha+\beta)\lambda_{\max}(P_0)^2 - \epsilon\lambda_{\max}(P_0) + \sigma_{max}(OT) < 0$. In order to find the conditions such that item (iv) in Proposition 8 is satisfied, let us solve the inequality with the variable $\hat{\theta}$ as follows:

$$(\alpha + \beta)\hat{\theta}^2 - \epsilon\hat{\theta} + \sigma_{\max}(OT) < 0 \tag{34}$$

The roots are

$$\hat{\theta}_1 = \frac{1}{2(\alpha+\beta)}\left(\epsilon - \sqrt{\epsilon^2 - 4(\alpha+\beta)\sigma_{\max}(OT)}\right), \quad \hat{\theta}_2 = \frac{1}{2(\alpha+\beta)}\left(\epsilon + \sqrt{\epsilon^2 - 4(\alpha+\beta)\sigma_{\max}(OT)}\right)$$

Based on the solution of the quadratic inequality (34), and following the condition of item (iv) in Proposition 8, $\lambda_{\max}(P_0)$ must satisfy the condition

$$\hat{\theta}_1 < \lambda_{\max}(P_0) < \hat{\theta}_2 \tag{35}$$

where the roots $\hat{\theta}_1$ and $\hat{\theta}_2$ are real and positive if the discriminant: $\epsilon^2 - 4(\alpha + \beta)\sigma_{\max}(OT) \geq 0$, given that $\alpha + \beta > 0$. It is possible to find $\lambda_{\max}(P_0)$ satisfying

(35) by properly constraining α and β, consequently constraining the uncertainty $\Delta\mu$. Additionally, ϵ can be chosen to determine the control gain K_0, which determines $\sigma_{\max}(OT)$.

Thus, this item (*i.e.*, $\hat{Q} \succcurlyeq \hat{S}\hat{R}^{\dagger}\hat{S}^{\top}$) is satisfied such that all the conditions in Proposition 8 holds as explained above.

Therefore, the matrix inequality $\hat{L} \succcurlyeq 0$ in (32) holds. Given that $\frac{4\Delta\mu^2 g^2 d}{df-e^2} \leq 1$ derived from the bound on ΔB in (31) where $\hat{\Lambda}_B = \begin{pmatrix} d & e \\ e & f \end{pmatrix} \succ 0$, let us assume that $||\Delta E'||^2 \leq \rho$ where $\rho = \frac{df-e^2}{4d}$. Thus, the inequality in (30) is written as:

$$\begin{aligned} \dot{V} &\leq -\begin{pmatrix} e \\ \Delta\lambda \end{pmatrix}^{\top} \left(-M_0 + \Delta M_0 - \begin{pmatrix} P_0\hat{\Lambda}_1 P_0 & 0 \\ 0 & 0 \end{pmatrix} \right) \begin{pmatrix} e \\ \Delta\lambda \end{pmatrix} + \Delta E'^{\top}\hat{\Lambda}_1^{-1}\Delta E' \\ &\leq -\epsilon' e^{\top} P_0 e + E'^{\top}\hat{\Lambda}_1^{-1}\Delta E' \\ &\leq -\epsilon'\lambda_{\min}(P_0)||e||^2 + \lambda_{\min}^{-1}(\hat{\Lambda}_1)||\Delta E'||^2 \leq -\epsilon'\lambda_{\min}(P_0)||e||^2 + \lambda_{\min}^{-1}(\hat{\Lambda}_1)\rho. \end{aligned} \tag{36}$$

So, $\dot{V} < 0$ outside the ball $B_r(0) \subset \mathbb{R}^n$, with $r \triangleq \sqrt{\frac{\lambda_{\min}^{-1}(\hat{\Lambda}_1)\rho}{\lambda_{\min}(P_0)\epsilon'}}$. Thus, the solution of (26) is GUUB [40, 24] by relaxing strong passivity and, according to [77, Proposition 4.5], the ultimate bound is given by:

$$||e|| \leq \sqrt{\frac{\lambda_{\max}(P_0)\lambda_{\min}^{-1}(\hat{\Lambda}_1)\rho}{\lambda_{\min}^2(P_0)\epsilon'}} \tag{37}$$

Remark 5 *It is important to note that taking $g_{21} = 0$ within the framework of bounded uncertainties in this section is not possible. This is due to the condition in item 1 ($\hat{R} \succcurlyeq 0$) to ensure that the matrix inequality $\hat{L} \succcurlyeq 0$ in (32) holds. Furthermore, it is necessary to select $g_{21} \geq \frac{1}{2}$ as imposed by item 1 in the above analysis. It is also worth noting that nowhere is used the fact that the set-valued part in right-hand side of (8) or (9) (equivalently, the multiplier λ_1) is bounded. The feedback controller structure respects the passivity-based structure as designed in [77].*

6.2 Numerical simulations

Let us check on an example if there exists P_0, K_0 and G_0 such that the BMI:

$$M_0 \preccurlyeq \begin{pmatrix} -\epsilon P_0 & 0 \\ 0 & 0 \end{pmatrix}, \tag{38}$$

holds where M_0 is defined in (27). For numerical purposes the BMI in (38) is transformed into an LMI (see appendix A.1). Take $\mu_0 = 0.5, m = 1$, $g = 9.8$, and $\epsilon = 10$. The software package MOSEK 9.3.14 [1] computes a solution given by:

$$K_0 = \begin{pmatrix} -70.79 & -11.95 \\ -29.89 & -4.22 \end{pmatrix}, \quad G_0 = \begin{pmatrix} 0 & 0 \\ 0.67 & 0 \end{pmatrix} \quad \text{and} \quad P_0 = \begin{pmatrix} 31.8 & 3.05 \\ 3.05 & 0.53 \end{pmatrix} \tag{39}$$

In order to find the admissible $\Delta\mu$, let us solve the LMI of uncertainties $\hat{L} \succcurlyeq 0$ in (32) with the unknowns $\hat{\Lambda}_1$ and $\hat{\Lambda}_B$ given the values of K_0, P_0 and G_0 from the strict passivity of the nominal system $(A_0 + E_0K_0, B_0, C_0 + F_0K_0, D_0 + F_0G_0)$. The solution is:

$$\hat{\Lambda}_1 = \begin{pmatrix} 0.16 & 0 \\ 0 & 9.2 \end{pmatrix} \quad \text{and} \quad \hat{\Lambda}_B = \begin{pmatrix} 0.14 & 0 \\ 0 & 0.567 \end{pmatrix} \tag{40}$$

with the constraint $\text{trace}(\hat{\Lambda}_1) \leq 10$ and without constraining $\hat{\Lambda}_B$. The admissible value of the upperbound on the uncertainty is $\Delta\mu \leq 0.038$. It is possible to increase the admissible $\Delta\mu$ for the same ϵ by increasing the values of $\hat{\Lambda}_1$ or $\hat{\Lambda}_B$ (*i.e.*, increasing the trace of the matrices $\hat{\Lambda}_1$ and $\hat{\Lambda}_B$), maintaining the BMI $\hat{L} \succcurlyeq 0$. Let us increase the value of $\hat{\Lambda}_B$ consequently $\Delta\mu$ such that $\text{trace}(\hat{\Lambda}_B) = 20$, the numerical solution is:

$$\hat{\Lambda}_1 = \begin{pmatrix} 0.032 & 0 \\ 0 & 0.86 \end{pmatrix} \quad \text{and} \quad \hat{\Lambda}_B = \begin{pmatrix} 0.023 & 0 \\ 0 & 19.9 \end{pmatrix} \tag{41}$$

The admissible value of the uncertainty is bounded such that $\Delta\mu \leq 0.22$. The following figure illustrates the robustness of the closed-loop error system (16) through simulations, considering perturbation on the parameter μ_0 by time-varying and bounded uncertainty $\Delta\mu$. Take $x_d(0) = (1, 0)^\top$, $x(0) = (0, -1)^\top$, and the time step $h = 0.01$s (simulations are still obtained using the time-stepping method available in SICONOS [2, 3]).

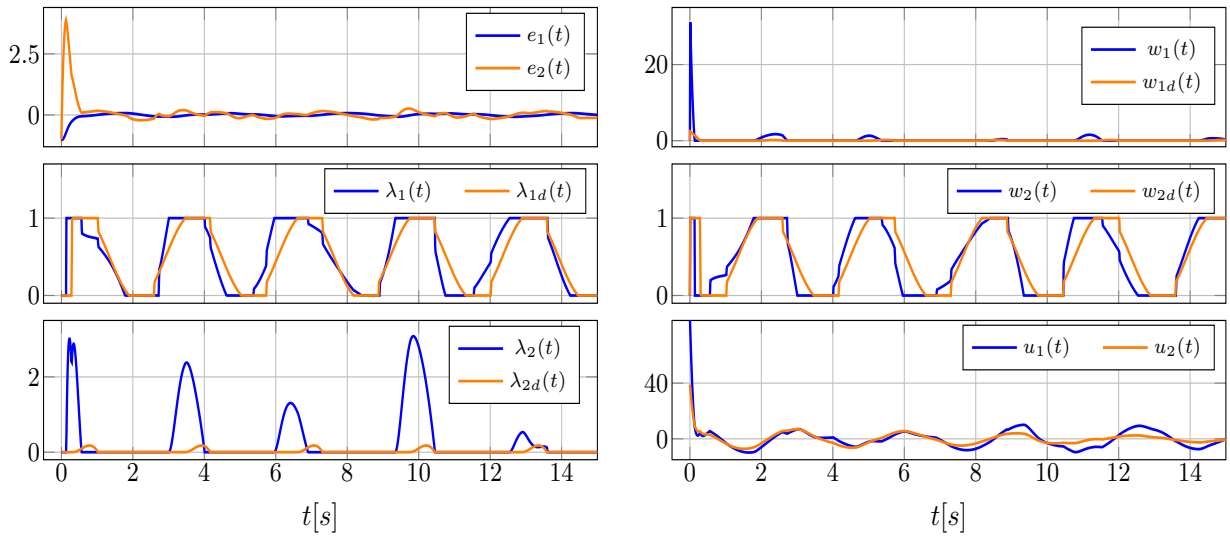

Figure 4: Closed-loop error system with control gains from (39) and uncertainty $\Delta\mu(t) = 0.2 \sin \sqrt{3}t$.

In Figure 4, the value of the uncertainty $\Delta\mu$ is bounded such that $\Delta\mu < 0.22$. The numerical simulation shows that the L_∞ norms of the error $e = x - x_d$ are $||e_1||_{[5,15],\infty} = 0.028$ and $||e_2||_{[5,15],\infty} = 0.154$. It is also noticeable that the synchronization between the complementarity variables λ and λ_d, as well as between w and w_d is lost in the presence of uncertainties.

7 Controller Design and Analysis with Stribeck Effects

As usual in control theory, it is interesting to analyse whether or not refining the model yields better results than designing a robust feedback controller. The foregoing study guarantees some robustness with respect to time-varying bounded uncertainties in the friction coefficient. Now, let us assume that the Coulomb's model is enhanced to include Stribeck effects. The reason of this assumption is that on one hand, Stribeck effects often represent in a quite acceptable way the frictional effects, on the other hand it will allow us to propose different control approach, using its hypomonotonicity (see Definition 2). Actually, any other modification of Coulomb's set-valued model which satisfies a hypomonotonicity constraint, would fit with the control framework in this section. This new approach consists of passifying (or "monotonifying") a hypomonotone friction model. As noted in the introduction, Stribeck effects often play a major role in practice.

7.1 The Stribeck Model and its Properties

One example of a physical model that may be considered as a bounded uncertainty, is the Stribeck model of sliding friction [6], which states that $\mu = \mu(\dot{q}_{rel})$, where $\dot{q}_{rel} \triangleq \dot{q} - u_2$ is the relative tangential velocity. It can be expressed as [14, Equation (17)]:

$$F_{\text{str}}(\dot{q}_{rel}(t)) = \underbrace{-F_{\text{n}}(\mu_s - \mu_c)\left(\exp\left(-\frac{\dot{q}_{rel}^2(t)}{v_s^2}\right) - 1\right)\text{sgn}(\dot{q}_{rel}(t))}_{F_{diff}(\dot{q}_{rel})} \underbrace{-\mu_s F_{\text{n}}\text{sgn}(\dot{q}_{rel}(t))}_{F_{sv}(\dot{q}_{rel}(t))}, \quad (42)$$

where $\mu_s > \mu_c > 0$, v_s are parameters, $F_{\text{n}} = mg > 0$ is the constant normal contact force. The total force is therefore the sum of a continuously differentiable, Lipschitz continuous, hypomonotone decreasing term $F_{diff}(\dot{x})$, and a set-valued maximal monotone term $F_{sv}(\dot{x})$. Figure 5 shows the graphical representations of different frictional forces, including Coulomb friction as F_{sv} and Stribeck friction F_{str} in (42) with respect to the relative velocity $\dot{q}_{rel}$. The behaviour of the function F_{diff} is depicted with variations in its parameter v_s. Take $F_n = mg = 9.8$, $\mu_s = 0.5$ and $\mu_c = 0.4$.

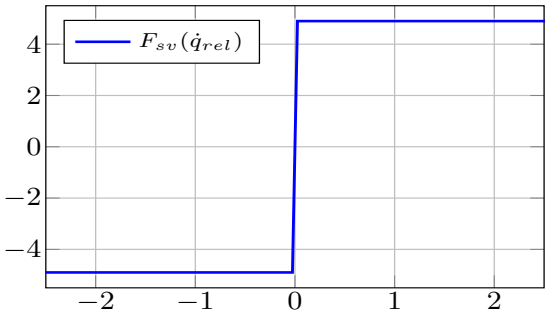

(a) Coulomb friction function

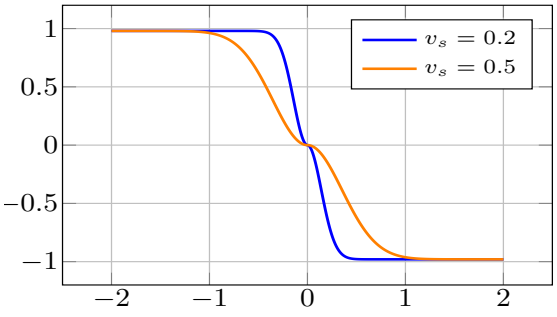

(b) Frictional force $F_{diff}(\dot{q}_{rel})$

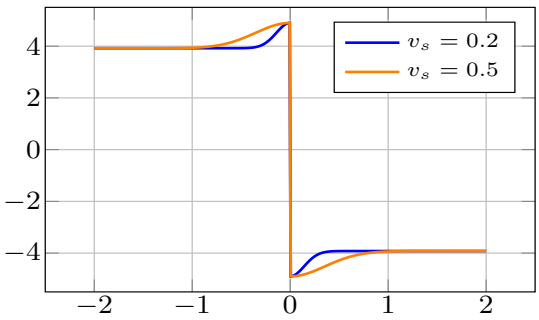

(c) Stribeck without viscous friction $F_{str}(\dot{q}_{rel})$

Figure 5: Different frictional forces as a function of relative velocity $\dot{q}_{rel}$

The plot in Figure 5a shows the Coulomb friction force with respect to the relative velocity $\dot{q}_{rel}$. It varies inside $F_{sv} \in [-F_n\mu_s, F_n\mu_s]$. In Figure 5b, the function F_{diff} is depicted for two parameters v_s, and $F_{diff} \in [-F_n(\mu_s - \mu_c), F_n(\mu_s - \mu_c)]$. The plot in Figure 5c displays the Stribeck friction force F_{str} without viscous friction as in (42) for two different values of the parameter v_s which causes faster decay towards the value $F_n(\mu_s - \mu_c)$ as it decreases. Let us analyze the behaviour of the function $F_{diff}(\dot{q}_{rel})$. Denote $\dot{q}_{rel}$ as x for simplicity, then the function $F_{diff}(x)$ is expressed as follows:

$$F_{diff}(x(t)) = F_n(\mu_s - \mu_c)\left(\exp\left(-\frac{x^2(t)}{v_s^2}\right) - 1\right)\operatorname{sgn}(x(t)).$$

The derivative of $F_{diff}(x)$ with respect to x is given for $x \neq 0$ by:

$$\frac{d}{dx}F_{diff}(x) = F_n(\mu_s - \mu_c)\left(-\frac{2x}{v_s^2}\exp\left(-\frac{x^2}{v_s^2}\right)\right)\operatorname{sgn}(x)$$

For $x > 0$: $\frac{d}{dx}F_{diff}(x) = -F_n(\mu_s - \mu_c)\frac{2x}{v_s^2}\exp\left(-\frac{x^2}{v_s^2}\right)$. For $x < 0$: $\frac{d}{dx}F_{diff}(x) = F_n(\mu_s - \mu_c)\frac{2x}{v_s^2}\exp\left(-\frac{x^2}{v_s^2}\right)$. Then, $\lim_{x\to 0^-}\frac{d}{dx}F_{diff}(x) = \lim_{x\to 0^+}\frac{d}{dx}F_{diff}(x) = 0$. Thus, the function $\frac{d}{dx}F_{diff}(\cdot)$ is continuous at 0, and the function $F_{diff}(\cdot)$ is continuously differentiable everywhere, with bounded derivatives (bounded in absolute value). It follows that it is a hypomonotone single-valued mapping. Let us write the dynamics in (8) with Stribeck friction presented in (42), then:

$$\ddot{q}(t) \in \frac{1}{m}u_1(t) - \mu g\,\operatorname{sgn}(\dot{q}_{rel}(t)) - F_{diff}(\dot{q}_{rel}(t)) \pm \alpha\dot{q}_{rel}(t) \tag{43}$$

where the linear term $\alpha\dot{q}_{rel}$ is added and subtracted. Thus, the dynamics in (43) is written as follows:

$$\ddot{q}(t) \in \frac{1}{m}u_1'(t) - \mu g\,\operatorname{sgn}(\dot{q}_{rel}(t)) - (F_{diff} + \alpha \mathrm{I_d})(\dot{q}_{rel}(t)) \tag{44}$$

where $u_1 = u_1' - m\alpha\dot{q}_{rel}$ and I_d is the identity mapping. It is required to find a suitable gain $\alpha > 0$ such that the mapping $\dot{q}_{rel} \mapsto (F_{diff} + \alpha \mathrm{I_d})(\dot{q}_{rel})$ is monotone (it is maximal since it is single-valued). For this purpose, it is required to find the maximum slope of the function $F_{diff}(.)$. The second derivative of $F_{diff}(x)$ is:

$$\frac{d^2}{dx^2}F_{diff}(x) = \frac{2}{v_s^4}F_n(\mu_s - \mu_c)\left((2x^2 - v_s^2)\exp\left(\frac{-x^2}{v_s^2}\right)\right)\operatorname{sgn}(x). \tag{45}$$

Let $m_{\max}$ be the maximum slope of $F_{diff}(x)$ which is the absolute value of $\frac{d}{dx}F_{diff}(x)$ at $x = \frac{v_s}{\sqrt{2}}$ and is given by:

$$m_{\max} = \frac{2}{v_s\sqrt{2}}F_n(\mu_s - \mu_c)\exp\left(-\frac{1}{2}\right). \tag{46}$$

Thus, the monotonicity of the mapping $\dot{q}_{rel} \mapsto (F_{diff} + \alpha \mathrm{I_d})(\dot{q}_{rel})$ is guaranteed by choosing the gain α such that $\alpha > m_{\max}$. Take

$$\alpha = \sqrt{2}\exp(\frac{1}{2})m_{\max} = \frac{2}{v_s}F_n(\mu_s - \mu_c) \tag{47}$$

in the following.

Remark 6 *If viscous friction is included in the force of friction given in (42), then the dynamics in (44) is rewritten as:*

$$\ddot{q}(t) \in \frac{1}{m}u_1'(t) - \mu g\ sgn(\dot{q}_{rel}(t)) - (F_{diff} + k_v + \alpha \mathrm{I_d})(\dot{q}_{rel}(t))$$

where $k_v > 0$ is the coefficient of viscous friction. Given that $k_v > 0$, the term $k_v\dot{q}_{rel}$ increases the overall damping by k_v, thus enhancing the dissipativity of the system which is crucial for our analysis. The main effect of adding viscous friction is that the value of the compensating term α changes such that $\alpha > \frac{2}{v_s\sqrt{2}}F_n(\mu_s - \mu_c)\exp\left(-\frac{1}{2}\right) + k_v$. Therefore, it is important to note that the following analytical approach applies to the Stribeck effect in (42) with viscous friction.

7.2 Controller Calculation

Let a suitable α be calculated. The next step consists of applying the foregoing passivity-based (or monotonicity-based) technique to calculate $u = (u_1', u_2)^\top = K(x - x_d) + u_d$ with $x \triangleq (q, \dot{q})^\top$ as independent input, then we have $u_1 = u_1' - m\alpha(\dot{q} - u_2)$. Let us write the dynamics in (44) according to the expression of F_{diff} in (42) as:

$$\begin{aligned}\ddot{q}(t) \ &\in \tfrac{1}{m}u_1'(t) - g\lambda_t\left(\mu_s + (\mu_s - \mu_c)\left(\exp\left(\tfrac{-(\dot{q}(t)-u_2(t))^2}{v_s^2}\right) - 1\right)\right) - \alpha(\dot{q}(t) - u_2(t)) \\ &= \tfrac{1}{m}u_1'(t) - g\mu_s\lambda_t - F_{diff,\alpha}(\dot{q} - u_2),\end{aligned}$$

where $\lambda_t \in \mathrm{sgn}(\dot{q} - u_2)$ and

$$F_{diff,\alpha}(\dot{q}_{rel}(t)) \triangleq (F_{diff} + \alpha \mathrm{I_d})(\dot{q}_{rel}(t)) = F_n(\mu_s - \mu_c)\left(\left(\exp\left(\tfrac{-(\dot{q}_{rel})^2}{v_s^2}\right) - 1\right) + \tfrac{2}{v_s}\right)(\dot{q}_{rel}(t))$$

is maximal monotone, where α is given in (47). Let us keep the plant dynamics as in (44) and write the desired dynamics in (14) with Stribeck friction in (42) as:

$$\begin{aligned}\ddot{q}_d(t) \ &\in \tfrac{1}{m}u_{1d}(t) - \mu_s g\mathrm{sgn}(\dot{q}_{rel,d}(t)) - F_{diff}(\dot{q}_{rel,d}(t)) \pm \alpha\dot{q}_{rel,d}(t) \\ &\in \tfrac{1}{m}u_{1d}'(t) - \mu_s g\mathrm{sgn}(\dot{q}_{rel,d}(t)) - (F_{diff} + \alpha I_d)(\dot{q}_{rel,d}(t))\end{aligned} \tag{48}$$

where $u_{1d}(t) = u'_{1d}(t) - m\alpha\dot{q}_{rel,d}(t)$ and $\dot{q}_{rel,d}(t) \stackrel{\Delta}{=} \dot{q}_d(t) - u_{2d}(t)$. The mapping $\dot{q}_{rel,d}(t) \mapsto F_{diff,\alpha}(\dot{q}_{rel,d}(t)) \stackrel{\Delta}{=} (F_{diff} + \alpha \mathrm{I_d})(\dot{q}_{rel,d}(t))$ is maximal monotone.

$\rightsquigarrow$ *Therefore, the Stribeck model is incorporated into the desired dynamics.* In view of the philosophy followed in this section, this is a logical step.

7.3 Error Dynamics Stability Analysis

Using (48) and (44), the error $\ddot{\tilde{q}} = \ddot{q} - \ddot{q}_d$ is written as:

$$\begin{aligned}
\ddot{\tilde{q}}(t) \quad &\in \tfrac{1}{m}(u_1(t) - u_{1d}(t)) - \mu_s g \mathrm{sgn}(\dot{q}_{rel}(t)) + \mu_s g \mathrm{sgn}(\dot{q}_{rel,d}(t)) - F_{diff,\alpha}(\dot{q}_{rel}(t)) \\
&\quad + F_{diff,\alpha}(\dot{q}_{rel,d}(t)) \\
&\in \tfrac{1}{m}(u'_1(t) - m\alpha(\dot{q}_{rel}(t) - \dot{q}_{rel,d}(t)) - u'_{1d}(t)) - \mu_s g(\mathrm{sgn}(\dot{q}_{rel}(t)) - \mathrm{sgn}(\dot{q}_{rel,d}(t))) \\
&\quad - (F_{diff,\alpha}(\dot{q}_{rel}(t)) - F_{diff,\alpha}(\dot{q}_{rel,d}(t))) \\
&\in \tfrac{1}{m}\left(k_{11}(q(t) - q_d(t)) + k_{12}(\dot{q}(t) - \dot{q}_d(t)) - m\alpha(\dot{q}(t) - k_{21}(q(t) - q_d(t))\right. \\
&\quad \left. - k_{22}(\dot{q}(t) - \dot{q}_d(t)) - \dot{q}_d(t)\right) \\
&\quad - \mu_s g(\mathrm{sgn}(\dot{q}_{rel}(t)) - \mathrm{sgn}(\dot{q}_{rel,d}(t))) - (F_{diff,\alpha}(\dot{q}_{rel}(t)) - F_{diff,\alpha}(\dot{q}_{rel,d}(t)))
\end{aligned} \tag{49}$$

with $\tilde{q} = q - q_d$ and $e = (\tilde{q}, \dot{\tilde{q}})^\top$. The error dynamics in (49) is equivalently written as:

$$\begin{aligned}
\dot{e}(t) \quad &\in \underbrace{\left(A_{cl} + \begin{pmatrix} 0 \\ \alpha \end{pmatrix} (C_{cl})_{1,\bullet}\right)}_{\stackrel{\Delta}{=} \hat{A}_{cl}} e(t) - \begin{pmatrix} 0 \\ \mu_s g \end{pmatrix} (\mathrm{sgn}(\dot{q}_{rel}(t)) - \mathrm{sgn}(\dot{q}_{rel,d}(t))) \\
&\quad - \begin{pmatrix} 0 \\ F_{diff,\alpha}(\dot{q}_{rel}(t)) - F_{diff,\alpha}(\dot{q}_{rel,d}(t)) \end{pmatrix}
\end{aligned} \tag{50}$$

where $\lambda_{1d}(t) \in \mathrm{sgn}(\dot{q}_d(t) - u_{2d}(t))$, $\lambda_1(t) \in \mathrm{sgn}(-(C_{cl})_{1,\bullet} e(t) + \dot{q}_d(t) - u_{2d}(t))$.

Proposition 4 *Consider the error dynamics in (50) with bounded initial conditions, and assume that the quadruple $(\hat{A}_{cl}, B_{cl}, C_{cl}, D_{cl})$ of the closed loop system is strictly state passive with $\epsilon > 0$. Then, the equilibrium point $e^\star = 0$ is globally exponentially stable.*

Consider the error dynamics in (50). Assume that the new closed-loop quadruple $(\hat{A}_{cl}, B_{cl}, C_{cl}, D_{cl})$ is strictly state passive. This means that the following matrix inequality:

$$\begin{pmatrix} \hat{A}_{cl}^\top \hat{P} + \hat{P}\hat{A}_{cl} & \hat{P}B_{cl} - C_{cl}^\top \\ B_{cl}^\top \hat{P} - C_{cl} & -D_{cl} - D_{cl}^\top \end{pmatrix} \preccurlyeq \begin{pmatrix} -\epsilon \hat{P} & 0 \\ 0 & 0 \end{pmatrix} \tag{51}$$

has a solution with $\hat{P} = \hat{P}^\top \succ 0$. Note that this BMI is transformed into LMI (see appendix A.1) to be solved numerically. Consider the storage function $V(e(t)) = e^\top(t)\hat{P}e(t)$. The rate of change of the storage function is:

$$\begin{aligned}\dot{V}(e(t)) &= e^\top(\hat{A}_{cl}^\top\hat{P} + \hat{P}\hat{A}_{cl})e + 2e^\top\hat{P}\begin{pmatrix}0\\ \mu_s g\end{pmatrix}\left[\mathrm{sgn}(\dot{q}_{rel,d}(t)) - \mathrm{sgn}(\dot{q}_{rel}(t))\right] \\ &\quad -2e^\top\hat{P}\begin{pmatrix}0\\ F_{diff,\alpha}(\dot{q}_{rel,d}) - F_{diff,\alpha}(\dot{q}_{rel})\end{pmatrix}\end{aligned}$$

Take $\hat{P} = \begin{pmatrix}\hat{p}_{11} & \hat{p}_{12}\\ \hat{p}_{21} & \hat{p}_{22}\end{pmatrix}$. Given that $\hat{P}B_{cl} = C_{cl}$ holds and that $(C_{cl})_{1,\bullet}e(t) = u_2(t) - \dot{q}(t) - u_{2d}(t) + \dot{q}_d(t)$, then the rate of change of the storage function is written as follows:

$$\begin{aligned}\dot{V}(e) &= e^\top(\hat{A}_{cl}^\top\hat{P} + \hat{P}\hat{A}_{cl})e - e^\top(\hat{P}B_{cl})_{\bullet,1}\left[\mathrm{sgn}(\dot{q}_{rel,d}(t)) - \mathrm{sgn}(\dot{q}_{rel}(t))\right] \\ &\quad -\tfrac{1}{\mu_s g}e^\top(\hat{P}B_{cl})_{\bullet,1}\left[F_{diff,\alpha}(\dot{q}_{rel,d}) - F_{diff,\alpha}(\dot{q}_{rel})\right] \\ &= e^\top(\hat{A}_{cl}^\top\hat{P} + \hat{P}\hat{A}_{cl})e + e^\top(C_{cl}^\top)_{\bullet,1}\left[\mathrm{sgn}(\dot{q}_{rel}(t)) - \mathrm{sgn}(\dot{q}_{rel,d}(t))\right] \\ &\quad +\tfrac{1}{\mu_s g}e^\top(C_{cl}^\top)_{\bullet,1}\left[F_{diff,\alpha}(\dot{q}_{rel}) - F_{diff,\alpha}(\dot{q}_{rel,d})\right] \qquad (52) \\ &= e^\top(\hat{A}_{cl}^\top\hat{P} + \hat{P}\hat{A}_{cl})e - \left[\dot{q}_{rel}(t) - \dot{q}_{rel,d}(t)\right]^\top\left[\mathrm{sgn}(\dot{q}_{rel}(t)) - \mathrm{sgn}(\dot{q}_{rel,d}(t))\right] \\ &\quad - \left[\dot{q}_{rel}(t) - \dot{q}_{rel,d}(t)\right]^\top\left[F_{diff,\alpha}(\dot{q}_{rel}) - F_{diff,\alpha}(\dot{q}_{rel,d})\right] \\ &\leq e^\top(\hat{A}_{cl}^\top\hat{P} + \hat{P}\hat{A}_{cl})e \leq -\epsilon e(t)^\top\hat{P}e(t)\end{aligned}$$

Therefore, the equilibrium point of the error dynamics in (50), $e^\star = 0$, is globally exponentially stable due to the fact: $\|e(t)\|^2 \leq \frac{V(0)}{\lambda_{\min}(\hat{P})}\exp(-\epsilon t)$.

Remark 7 *The above tracking controller aims at improving the closed-loop accuracy when the friction effects follow Stribeck's model and the parameters are correctly identified. Other control strategies are possible and not tackled here. For instance, the term $F_{diff}(\dot{q}_{rel})$ is uniformly bounded and thus could be compensated for with a simple first-order sliding-mode input, hence dispensing the designer for the knowledge of parameters μ_c and v_s (see (42)). This would however be at the price of applying an input u_1 which is no longer a feedforward input (in case $k > 0$ and $f > 0$). It would also allow us to design another desired system, as in (48) without the nonlinear term $F_{diff}(\dot{q}_{rel,d}(t))$. For the sake of briefness this is not developed further.*

7.4 Numerical simulation

Recall that $x \triangleq (q, \dot{q})$, $x_d \triangleq (q_d, \dot{q}_d)$, and $e \triangleq (\tilde{q}, \dot{\tilde{q}})$. The desired dynamics in (48), the closed-loop dynamics in (44) and the error dynamics in (50) can be equivalently expressed in the form of LCS as explained in section 3.1. The following numerical simulation is obtained using the LCS time-stepping scheme available in SICONOS [2, 3]. Take $m = 1\text{kg}$, $F_n = mg = 9.8\text{m/s}^2, v_s = 0.2, \mu_s = 0.5$ and $\mu_c = 0.4$. Let us check if there exists a control gain K such that the closed-loop system's quadruple $(A + EK, B, C + FK, D)$ is strictly state passive. The LMI derived from the BMI of strict state passivity in (17) has a solution which is given by:

$$K = \begin{pmatrix} -70.79 & -11.95 \\ -23.91 & -3.18 \end{pmatrix} \quad \text{and} \quad P = \begin{pmatrix} 31.8 & 3.05 \\ 3.05 & 0.53 \end{pmatrix}$$

Consider the value of the linear term α in (47), and the controller $u_1 = k_{11}(x_1 - x_{1d}) + k_{12}(x_2 - x_{2d}) + u_{1d} - m\alpha(x_2 - u_2)$ and $u_2 = k_{21}(x_1 - x_{1d}) + k_{22}(x_2 - x_{2d}) + u_{2d}$. The initial conditions are $x_d(0) = (-1, -2)^\top$ and $x(0) = (1, 3)^\top$, with desired inputs $u_{1d} = 0.7m\mu g \cos 5t$ and $u_{2d} = 0.5m\mu g \sin 3t$, and a time step $h = 0.01\text{s}$.

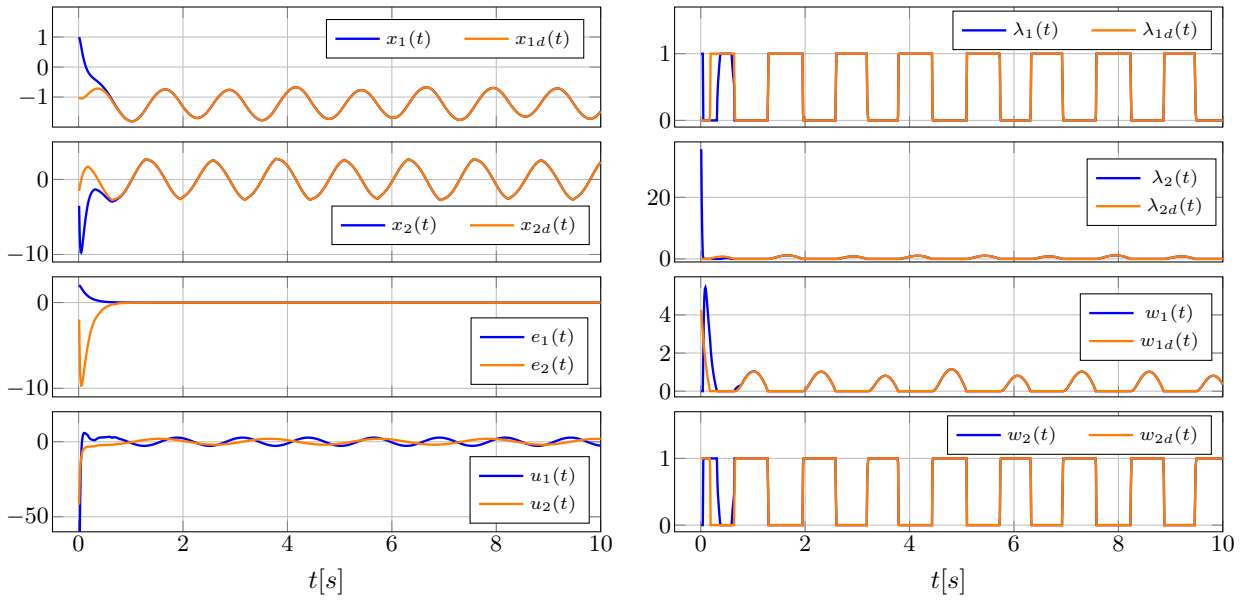

Figure 6: The desired, closed-loop and error systems of the LCS in (44), complementarity variables (λ, w) and input $u = (u_1, u_2)^\top$.

The numerical simulation shows the desired trajectories generated by (48). The numerical simulation in Figure 6 shows that the tracking error e converges exponentially to zero, which confirms the result stated in Proposition 4 when the friction model includes Stribeck effects. It can be observed that the plant's complementarity variables (λ, w) converge to the desired complementarity variables (λ_d, w_d).

8 Two-mass Oscillator: Center of Gravity Tracking Control

This section is dedicated to analyze an extension of the above oscillator, when several (here, two) masses are sliding on the belt.

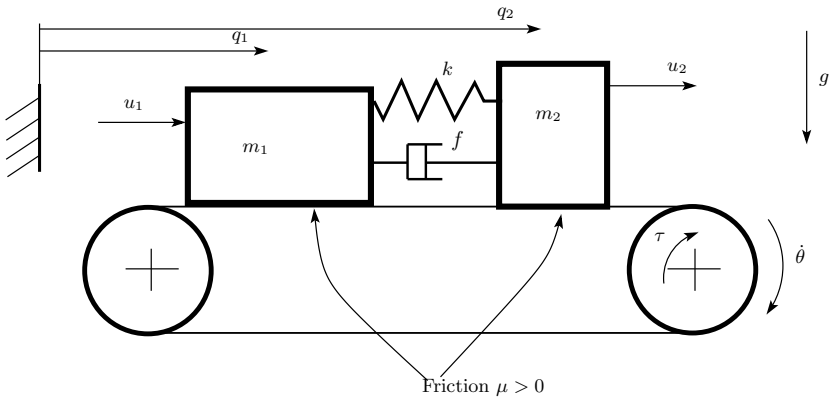

Figure 7: Frictional oscillator with two masses.

8.1 Center of Mass' Dynamics

Let us now consider the extension of (9) as depicted in Fig. 7:

$$\begin{cases} (a)\ \ddot{q}_1(t) \in \frac{u_1(t)}{m_1} - \frac{k}{m_1}(q_1 - q_2) - \frac{f}{m_1}(\dot{q}_1 - \dot{q}_2) - \mu_1 g\ \mathrm{sgn}(\dot{q}_1(t) - r\dot{\theta}(t)) \\ (b)\ \ddot{q}_2(t) \in \frac{u_2(t)}{m_2} + \frac{k}{m_2}(q_1 - q_2) + \frac{f}{m_2}(\dot{q}_1 - \dot{q}_2) - \mu_2 g\ \mathrm{sgn}(\dot{q}_2(t) - r\dot{\theta}(t)) \\ (c)\ I\ddot{\theta}(t) \in \tau(t) + r\mu_1 m_1 g\ \mathrm{sgn}(\dot{q}_1(t) - r\dot{\theta}(t)) + r\mu_2 m_2 g\ \mathrm{sgn}(\dot{q}_2(t) - r\dot{\theta}(t)), \end{cases} \tag{53}$$

This yields:

$$\begin{cases} (m_1 + m_2)\ddot{q}_c(t) \in u_1(t) + u_2(t) - \mu_1 m_1 g \mathrm{sgn}(\dot{q}_1(t) - r\dot{\theta}(t)) - \mu_2 m_2 g\ \mathrm{sgn}(\dot{q}_2(t) - r\dot{\theta}(t)) \\ I\ddot{\theta}(t) \in \tau(t) + r\mu_1 m_1 g\ \mathrm{sgn}(\dot{q}_1(t) - r\dot{\theta}(t)) + r\mu_2 m_2 g\ \mathrm{sgn}(\dot{q}_2(t) - r\dot{\theta}(t)), \end{cases} \tag{54}$$

with $q_c \triangleq \frac{m_1 q_1 + m_2 q_2}{m_1 + m_2}$ the masses' center of gravity position. After some manipulations we obtain:

$$\begin{cases} (m_1 + m_2)\ddot{q}_c(t) \in u_1(t) + u_2(t) - \mathcal{F}_{\mathrm{t}}(-u_3) \\ I\ddot{\theta}(t) \in \tau(t) + r\mathcal{F}_{\mathrm{t}}(-u_3) \end{cases} \tag{55}$$

where the mapping $-u_3 \mapsto \mathcal{F}_{\rm t}(-u_3) = \mu_1 m_1 g \ \mathrm{sgn}(\dot{q}_1 - u_3) + \mu_2 m_2 g \ \mathrm{sgn}(\dot{q}_2 - u_3)$, $u_3 = r\dot{\theta}$, is maximal monotone [8, Corollary 24.4]. It can be computed as a set-valued piecewise-constant mapping:

$$\begin{cases} -\mu_1 m_1 g - \mu_2 m_2 g & \text{if } u_3 > \dot{q}_2(t) > \dot{q}_1(t) \\ \mu_1 m_1 g + \mu_2 m_2 g & \text{if } u_3 < \dot{q}_1(t) < \dot{q}_2(t) \\ -\mu_1 m_1 g + \mu_2 m_2 g & \text{if } \dot{q}_1(t) < u_3 < \dot{q}_2(t) \\ [-\mu_1 m_1 g - \mu_2 m_2 g, -\mu_1 m_1 g + \mu_2 m_2 g] & \text{if } u_3 = \dot{q}_2(t) \\ [-\mu_1 m_1 g + \mu_2 m_2 g, \mu_1 m_1 g + \mu_2 m_2 g] & \text{if } u_3 = \dot{q}_1(t) \end{cases} \tag{56}$$

and similarly if $\dot{q}_1(t) > \dot{q}_2(t)$. For each fixed t there exists a convex proper continuous function $f_{\rm t}(\cdot)$ such that $\mathcal{F}_{\rm t}(-u_3) = \partial f_{\rm t}(-u_3)$, where ∂ is the subdifferentiation of Convex Analysis (see Definition 3). The analogy between (9) and (55) (56) is clear. Therefore, the same control strategy can be applied to (55) (56) for trajectory tracking control of the center of mass position and velocity. To this aim only one input u_1 or u_2 is sufficient. Extension to $n \geq 3$ aligned blocks follows the same lines. One significant discrepancy compared with the one-mass oscillator, is that the desired dynamics when designed as above, depends on $\dot{q}_1$ and $\dot{q}_2$ since $\mathcal{F}_{\rm t}$ does. Indeed a natural choice is:

$$(m_1 + m_2)\ddot{q}_{cd}(t) \in u_{1d}(t) - \mathcal{F}_{\rm t}(-u_{3d}(t)), \tag{57}$$

where $q_{cd} : \mathbb{R}_+ \to \mathbb{R}$ is the desired center of mass motion. This allows us to redo the analysis in the previous sections. However, it is noteworthy that contrarily to (13), the dynamics (57) is not autonomous, thus the design of $q_{cd}(\cdot)$ is not possible from it. The problem is more a synchronization problem between (57) and (55) than a trajectory control problem. To cope with this issue we may design the desired system as follows, where the dependence of $\mathcal{F}_{\rm t}$ on $\dot{q}_1$ and $\dot{q}_2$ is replaced by dependence on signals $\dot{q}_{1d}$ and $\dot{q}_{2d}$. To that end let us rewrite (54) (equivalently (55) (56)) in its LCS form as (time argument is dropped):

$$\begin{aligned} \dot{x}_c &= \underbrace{\begin{pmatrix} 0 & 1 \\ 0 & 0 \end{pmatrix}}_{\triangleq A_c} x_c + \underbrace{\begin{pmatrix} 0 & 0 \\ \frac{1}{m_1+m_2} & 0 \end{pmatrix}}_{\triangleq E_c} u_c + \underbrace{\begin{pmatrix} 0 & 0 & 0 & 0 \\ \frac{-2\mu_1 g m_1}{m_1+m_2} & 0 & \frac{-2\mu_2 m_2 g}{m_1+m_2} & 0 \end{pmatrix}}_{\triangleq B_c} \lambda_c + \underbrace{\begin{pmatrix} 0 \\ \frac{(\mu_1 m_1 + \mu_2 m_2) g}{m_1+m_2} \end{pmatrix}}_{\triangleq E'_c} \\ 0 \leq \lambda_c \perp w_c &= \underbrace{\begin{pmatrix} 0 & 1 \\ 0 & 0 \\ 0 & 1 \\ 0 & 0 \end{pmatrix}}_{\triangleq F_c} u_c + \underbrace{\begin{pmatrix} 0 & 1 & 0 & 0 \\ -1 & 0 & 0 & 0 \\ 0 & 0 & 0 & 1 \\ 0 & 0 & -1 & 0 \end{pmatrix}}_{\triangleq D_c} \lambda_c + \underbrace{\begin{pmatrix} 0 & \frac{m_2}{m_1} \\ 0 & 0 \\ \frac{m_1}{m_2} & 0 \\ 0 & 0 \end{pmatrix}}_{\triangleq H_c} \begin{pmatrix} \dot{q}_1 \\ \dot{q}_2 \end{pmatrix} + F'_c + \underbrace{\begin{pmatrix} 0 & -\frac{m_1+m_2}{m_1} \\ 0 & 0 \\ 0 & -\frac{m_1+m_2}{m_2} \\ 0 & 0 \end{pmatrix}}_{\triangleq C_c} x_c \geq 0, \end{aligned} \tag{58}$$

with $x_c = (q_c \ \dot{q}_c)^\top$, $\lambda_c = (\lambda_1 \ \lambda_2 \ \lambda_3 \ \lambda_4)^\top$, $u_c = (u_{c1} \ u_{c2})^\top = (u_1 + u_2 \ u_3)^\top$, $F'_c = (0 \ 1 \ 0 \ 1)^\top$. The dependence of $\mathcal{F}_{\rm t}$ on velocities is visible through $H_c\dot{q}$, $\dot{q} = (\dot{q}_1 \ \dot{q}_2)^\top$. The idea is to define the desired dynamics using the complementarity constraint:

$$0 \leq \lambda_{cd} \perp w_{cd} = F_c u_{cd} + D_c \lambda_{cd} + C_c x_{cd} + F'_c + H_c \dot{q}_d \geq 0, \tag{59}$$

while the dynamical part is set as:

$$\dot{x}_{cd} = A_c x_{cd} + E_c u_{cd} + E'_c + B_c \lambda_{cd}. \tag{60}$$

Clearly $\dot{q}_{1d}$, $\dot{q}_{2d}$ and $\dot{q}_{cd}$ are not independent variables.

8.2 Closed-loop Error Dynamics and Stability Analysis

The error dynamics with $u_c = K(x_c - x_{cd}) + u_{cd}$ is given by:

$$\begin{cases} \dot{\tilde{x}}_c(t) = (A_c + E_c K)\tilde{x}_c(t) + B_c(\lambda_c(t) - \lambda_{cd}(t)) \\ \\ 0 \le \lambda_{cd}(t) \perp w_{cd}(t) = F_c u_{cd}(t) + D_c \lambda_{cd}(t) + C_c x_{cd}(t) \\ \qquad +F'_c + H_c \dot{q}_d(t) \ge 0 \\ \\ 0 \le \lambda_c(t) \perp w_c(t) = (C_c + F_c K)\tilde{x}_c(t) + F_c u_{cd}(t) \\ \qquad +C_c x_{cd} + D_c \lambda_c(t) + F'_c + H_c \dot{q}(t) \ge 0 \end{cases} \tag{61}$$

Proposition 5 *where $\tilde{x}_c = x_c - x_{cd}$. Assume that the quadruple $(A_c + E_c K, B_c, C_c + F_c K, D_c)$ is strictly state passive, and that $\dot{\tilde{q}}_1$ is bounded. Then $(\tilde{q}_c, \dot{\tilde{q}}_c)^\top$ is globally uniformly ultimately bounded, and $\dot{\tilde{q}}_2$ is bounded.*

Let $V_c(\tilde{x}_c) = \frac{1}{2}\tilde{x}_c^\top P_c \tilde{x}_c$, where $P_c = P_c^\top \succ 0$ is a solution of SSPMI$(A_c + E_c K, B_c, C_c + F_c K, D_c, \epsilon)$. We obtain along trajectories of (61):

$$\begin{aligned} \dot{V}_c(t) &= \tilde{x}_c^\top (P_c(A_c + E_c K) + (A_c + E_c K)^\top P_c)\tilde{x}_c + \tilde{x}_c^\top P_c B_c(\lambda_c - \lambda_{cd}) \\ &\le -\epsilon \tilde{x}_c^\top P_c \tilde{x}_c + \tilde{x}_c^\top (C_c + F_c K)(\lambda_c - \lambda_{cd}) \\ &\le -\epsilon \tilde{x}_c^\top P_c \tilde{x}_c + (w_c - w_{cd} + D_c(\lambda_{cd} - \lambda_c) - H_c \dot{\tilde{q}})^\top (\lambda_c - \lambda_{cd}) \\ &\le -\epsilon \tilde{x}_c^\top P_c \tilde{x}_c + (w_c - w_{cd} - H_c \dot{\tilde{q}})^\top (\lambda_c - \lambda_{cd}) \le -\epsilon \tilde{x}_c^\top P_c \tilde{x}_c - \dot{\tilde{q}}^\top H_c^\top (\lambda_c - \lambda_{cd}) \end{aligned} \tag{62}$$

From (58) and (54) it is inferred that $H_c^\top(\lambda_c - \lambda_{cd})$ is bounded, since it involves only λ_1 and λ_3 which are selections of signum functions. We also have $\dot{\tilde{q}}_c = \frac{(m_1 \ m_2)\dot{\tilde{q}}}{m_1 + m_2}$, $\tilde{x}_c = (\tilde{q}_c \ \dot{\tilde{q}}_c)^\top$. Thus:

$$\begin{aligned} \dot{V}_c(t) &\le -\epsilon \tilde{x}_c^\top P_c \tilde{x}_c + \sqrt{\mu_1^2 m_2^2 + \mu_2^2 m_1^2}\, g ||\dot{\tilde{q}}|| \\ &\le -\epsilon_1(\epsilon)\tilde{q}_c^2 - \epsilon_2(\epsilon)\dot{\tilde{q}}_c^2 + \epsilon_3(|\dot{\tilde{q}}_1| + |\dot{\tilde{q}}_2|) \\ &\le -\epsilon_1(\epsilon)\tilde{q}_c^2 - \epsilon_2(\epsilon)\dot{\tilde{q}}_c^2 + \epsilon_4|\dot{\tilde{q}}_1| + \epsilon_5|\dot{\tilde{q}}_c| \\ &\le -\epsilon_1(\epsilon)\tilde{q}_c^2 - \epsilon_2(\epsilon)|\dot{\tilde{q}}_c|(|\dot{\tilde{q}}_c| - \tfrac{\epsilon_4}{\epsilon_2(\epsilon)}) + \epsilon_4|\dot{\tilde{q}}_1|_{\max}, \end{aligned} \tag{63}$$

where ϵ_i are positive constants, $\epsilon_i(\epsilon) \to +\infty$ as $\epsilon \to +\infty$, $i = 1, 2$.

Remark 8 *It appears clearly in (62) why setting $H_c\dot{q}$ instead of $H_c\dot{q}_d$ in (59) simplifies the analysis. The price to pay is to prevent the generation of wanted desired trajectories.*

The inputs u_{c1} and u_3 can be used to design the above controller u_c. The input u_1 can be used to guarantee a bounded $\dot{q}_1$ in (53) (a). Then $u_2 = u_{c1} - u_1$. It is noteworthy that f and k in Figure 7 do not play any role in the above analysis and could be set to zero. However it plays a role in the boundedness of the first mass' state. Assume that $k = 0$ and $k = 0$. Then (53) (a) is rewritten as:

$$\ddot{q}_1(t) \in \frac{u_1(t)}{m_1} - \mu_1 g \, \mathrm{sgn}(\dot{q}_1(t) - r\dot{\theta}(t)) \tag{64}$$

The boundedness of $\dot{\tilde{q}}_1$ is guaranteed by any controller of the form $u_1 = -k_1(q_1 - q_{1d}) - f_1(\dot{q}_1 - \dot{q}_{1d}) + \ddot{q}_{1d}$. Similarly as in the one-mass system, the spring-dashpot terms can be realized passively by attaching the mass m_1 to the wall (see Figure 1b)), so that u_1 is a feedforward input $u_1(q_{1d}, \dot{q}_{1d}, \ddot{q}_{1d})$. Thus we arrived to the following.

Proposition 6 *Consider the two-mass system in (53), with $k = 0$, $f = 0$, and mass m_1 attached to the wall with a spring-dashpot with stiffness $k_1 > 0$, damping $f_1 > 0$. Let $u_1 = k_1 q_{1d} + f_1 \dot{q}_{1d} + \ddot{q}_{1d}$, $u_c = (u_{c1}, u_{c2})^\top = K(x_c - x_{cd}) + u_{cd}$, $u_2 = u_{c1} - u_1$, $u_{c2} = u_3$, and assume that the quadruple $(A_c + E_c K, B_c, C_c + F_c K, D_c)$ is strictly state passive with constant $\epsilon > 0$. Then the state of the error dynamics in (61) is globally uniformly ultimately bounded in a ball whose radius $r(\epsilon)$ strictly decreases as ϵ strictly increases. Moreover both $(q_1, \dot{q}_1)^\top$ and $(q_2, \dot{q}_2)^\top$ are bounded.*

The stiffness k_1 and the damping coefficient f_1 are attached between the wall and mass m_1, similarly as k and f in Fig. 1b.

Remark 9 *All systems in (8), (9), (10), (43), (58) and (55) (56) belong to set-valued Lur'e dynamical systems [16, 17] with controllers. A block-diagram representation is as in Fig. 8. In this article the set-valued feedback may be the signum function (8), (9), or an operator defined from complementarity constraints (10), or the multifunction in (56). The closed-loop error systems (16), (26), (50), (61) can also be recast in the set-valued Lur'e class of systems (without control inputs). It is conjectured that the material in this paper can be extended to more general classes of maximal monotone set-valued feedback mappings.*

9 Conclusions

This article deals with trajectory tracking control of frictional oscillators, which are low-dimensional strongly nonsmooth and set-valued systems made of a mass sliding on a moving belt. Passivity (feedback passification) and maximal monotonicity of the friction model are at the core of the stability analysis. The overall objective is not to compensate for friction

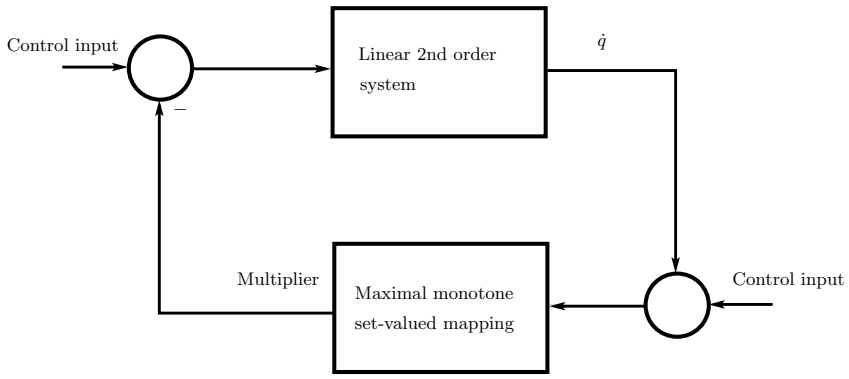

Figure 8: Block-diagram of the control and closed-loop systems.

before setting a tracking controller, but to use its monotonicity for control purposes. This is, to the best of authors' knowledge, an original approach. The problem is solved with 2-dimensional Coulomb's friction, both when the friction coefficient is known, and when uncertainties are present where robustness is carefully studied. It is extended to the case of varying friction coefficient (Stribeck's model), where the hypomonotonicity of the model is used. The case of two masses moving on a belt is studied, where the objective is to control the masses' center of gravity. Numerical simulations illustrate the theoretical results.

A Useful Mathematical Results

A.1 Transformation of BMI to an LMI

The bilinear matrix inequality BMI in (17) can be reformulated to an LMI [67, Example 5.5 p.136]. The left-hand and the right-hand sides of (17) are multiplied by $\begin{pmatrix} Q & 0 \\ 0 & I \end{pmatrix}$, where $Q \triangleq P^{-1}$, and let $N \triangleq KQ$. It follows that

$$\begin{pmatrix} QA^\top + AQ + N^\top E^\top + EN + \epsilon Q & B + EG - QC^\top - N^\top F^\top \\ B^\top + G^\top E^\top - CQ - FN & -D - FG - (D + FG)^\top \end{pmatrix} \preccurlyeq 0 \tag{65}$$

This LMI is a feasible problem and it is solved numerically in the new variables $Q = Q^T \succ 0$, G, and N where $K = NQ^{-1}$.

A.2 Conditions for Positive Semi-Definiteness

Lemma 1 *[12, Proposition 8.2.4, Remark after Fact 6.4.5] Consider the matrix* $M = \begin{pmatrix} Q & S \\ S^\top & R \end{pmatrix}$. *Assume that* $Q = Q^\top$ *and* $R = R^\top$. *Then, the matrix* M *is positive semi-*

definite (i.e. $M \succcurlyeq 0$) *if and only if:*

1. $R \succcurlyeq 0$,
2. $SR^\dagger R = S \Leftrightarrow \mathrm{Im}(S^\top) \subseteq \mathrm{Im}(R)$,
3. $Q \succcurlyeq SR^\dagger S^\top$.

[33] Let $\mathbb{R}^{m\times m} \ni M = M^\top \succ 0$, $x \in \mathbb{R}^m$, $q \in \mathbb{R}^m$ and $K \subseteq \mathbb{R}^m$ be a closed nonempty convex set. Then:

$$M(x-q) \in -\mathcal{N}_K(x) \Leftrightarrow x = \mathrm{proj}_M[K;q] \Leftrightarrow x = \mathrm{argmin}_{z\in K} \frac{1}{2}(z-q)^\top M(z-q), \tag{66}$$

where proj_M is the orthogonal projection in the metric defined by M. Moreover such a x is unique.

B Material on Relaxing Strong Passivity to Strict State Passivity

As noted earlier, the closed-loop system in (12) cannot be made strongly passive (see Remark 2). This motivates us to apply the theoretical results on relaxing the strong passivity property from [77, section 4.3]. Let us recall some of these results, which mainly rely on the positive semi-definiteness conditions presented in Definition 1.

Proposition 7 *[77, Proposition 4.4] Let Assumption 1 holds for the nominal system. Assume that $x_d : \mathbb{R}_+ \to \mathbb{R}^n$ is AC, $\lambda_d(u_d, x_d)$ is bounded, and that the closed-loop system in (25) is well-posed. Then, the matrix inequality*

$$-M_0 + \Delta M_0 - \begin{pmatrix} \epsilon' P_0 & 0 \\ 0 & 0 \end{pmatrix} - \begin{pmatrix} P_0\Lambda_1 P_0 & 0 \\ 0 & \Lambda_2 \end{pmatrix} \succcurlyeq 0 \tag{67}$$

where M_0 in (27) corresponds to the strict state passivity LMI with $\epsilon > 0$ and ΔM_0 is defined in section 6, holds for $\epsilon > \epsilon' > 0$ if and only if:

1. $R \triangleq (D_0 + F_0G_0) + (D_0 + F_0G_0)^\top + (\Delta D + \Delta F G_0) + (\Delta D + \Delta F G_0)^\top - \Lambda_2 \succcurlyeq 0$,
2. $Q \triangleq -(A_0 + E_0K_0 + \frac{\epsilon'}{2} I_n)^\top P_0 - P_0(A_0 + E_0K_0 + \frac{\epsilon'}{2} I_n) - (\Delta A + \Delta E K_0)^\top P_0 - P_0(\Delta A + \Delta E K_0) - P_0\Lambda_1 P_0 \succcurlyeq 0$, *with* $-(A_0 + E_0K_0)^\top P_0 - P_0(A_0 + E_0K_0) \succcurlyeq \epsilon P_0$, $\epsilon > \epsilon' > 0$,
3. $\mathrm{Im}(S^\top) \subseteq \mathrm{Im}(R)$, *with* $S \triangleq -P_0(B_0 + E_0G_0) + (C_0 + F_0K_0)^\top - P_0(\Delta B + \Delta E G_0) + (\Delta C + \Delta F K_0)^\top$,

4. $Q \succcurlyeq SR^{\dagger}S^{\top}$.

The following Lemma gives sufficient conditions for item 3 in Proposition 7 to be satisfied.

Lemma 2 *[77, Lemma 4.6] Let Assumption 1 hold for the nominal system. Assume that* $\mathrm{Im}(\Delta S^{\top}) \subseteq \mathrm{Im}(S_0^{\top})$, *and that* $\mathrm{Im}(R) = \mathrm{Im}(R_0)$, *then* $\mathrm{Im}(S^{\top}) \subseteq \mathrm{Im}(R)$.

The proposition below provides conditions on the uncertainty matrices to ensure that the inequality in item 4 holds when the nominal system is strictly state passive.

Proposition 8 *[77, Proposition 4.7] Let Assumption 1 hold for the quadruple* (A_0, B_0, C_0, D_0) *and define the matrix* OT *such that:*

$$\begin{aligned} OT = \; & S_0R_0^{\dagger}\Delta S^{\top} - S_0R_0^{\dagger}\Delta R R_0^{\dagger}S_0^{\top} - S_0R_0^{\dagger}\Delta R R_0^{\dagger}\Delta S^{\top} + \Delta S R_0^{\dagger}S_0^{\top} + \Delta S R_0^{\dagger}\Delta S^{\top} \\ & -\Delta S R_0^{\dagger}\Delta R R_0^{\dagger}S_0^{\top} - \Delta S R_0^{\dagger}\Delta R R_0^{\dagger}\Delta S^{\top}. \end{aligned}$$

Assume that: (i) $R \succcurlyeq 0$, *(ii)* $\mathrm{Im}(\Delta R) \subseteq \mathrm{Im}(R_0)$, *(iii)* $\mathrm{rank}(R_0) = r$, $R_0 \neq 0$, $\sigma_{\max}(\Delta R) < \sigma_r(R_0)$, *(iv)* $\sigma_{\max}(OT) + \sigma_{\max}(\mathcal{O}((R_0^{\dagger}\Delta R)^2)) + \sigma_{\max}(\Delta Q) < \epsilon\lambda_{\max}(P_0)$. *Then,* $Q \succcurlyeq SR^{\dagger}S^{\top}$.

C Stick/ Slip Behaviour of the Desired LCS in (13)

Recall the desired system in (13):

$$\begin{cases} \dot{x}_d(t) = \begin{pmatrix} 0 & 1 \\ 0 & 0 \end{pmatrix} x_d(t) + \begin{pmatrix} 0 & 0 \\ \frac{1}{m} & 0 \end{pmatrix} u_d(t) + \begin{pmatrix} 0 \\ \mu g \end{pmatrix} + \begin{pmatrix} 0 & 0 \\ -2\mu g & 0 \end{pmatrix} \lambda_d(t) \\ 0 \leq \lambda_d(t) \perp w_d(t) = \begin{pmatrix} 0 & 1 \\ 0 & 0 \end{pmatrix} u_d(t) + \begin{pmatrix} 0 \\ 1 \end{pmatrix} + \begin{pmatrix} 0 & 1 \\ -1 & 0 \end{pmatrix} \lambda_d(t) + \begin{pmatrix} 0 & -1 \\ 0 & 0 \end{pmatrix} x_d(t) \geq 0, \end{cases}$$

where $x_d = (q_d, \dot{q}_d)^{\top} = (x_{1d}, x_{2d})^{\top}$. According to the complementarity problem in (13), the multiplier $\lambda_{1d} \in [0, 1]$. Let us determine the value of the desired input u_{1d} for the different stick/ slip behaviour by considering the following analysis of the desired system in (13):

- If $\lambda_{1d} \in]0, 1[\Rightarrow x_{2d} = 0 \Rightarrow \dot{x}_{2d} = 0 \Rightarrow u_{1d} \in]-m\mu g, m\mu g[$. The system is in sticking mode.
- If $\lambda_{1d} = 0 \Rightarrow x_{2d} \leq 0$. When $u_{1d} = -m\mu g$, then $x_{2d} = 0$ and the system is in sticking mode. But, when $u_{1d}(t) < -m\mu g \;\; \forall t$, then the solution $x_{2d} < 0$ (*i.e.,* sliding mode) and it diverges.
- If $\lambda_{1d} = 1 \Rightarrow x_{2d} = \lambda_{2d} \geq 0$. When $u_{1d} = m\mu g$, then $x_{2d} = 0$ and the system behaves in sticking mode. When u_{1d} is chosen such that $u_{1d}(t) > m\mu g \;\; \forall t$, then the solution $x_{2d} > 0$, it behaves in sliding mode and it is unbounded.

  It is noteworthy that, in the cases when $\lambda_{1d} = 1$ or $\lambda_{1d} = 0$ (*i.e.,* $u_{1d} = m\mu g$ or $u_{1d} = -m\mu g$ respectively), and the initial velocity of the mass $x_{2d}(0)$ is chosen such that it is in the direction of the external force u_{1d} (*i.e.,* $u_{1d} < 0$ and $x_{2d}(0) < 0$). Then the trajectory x_{1d} diverges and it is sliding mode at a constant velocity.

If $u_{1d}(t)$ is chosen as a periodic, time-varying, and bounded signal in the form of $u_{1d} = Acos(wt)$ where $|A| > m\mu g$, then the system will behave in both sticking and sliding modes or non-sticking mode depending on the amplitude A.

D Equilibrium Points of the Closed-loop Error System in (16)

In order to find the equilibrium points of the error dynamics, the LCS in (16) is written as follows:

$$\begin{cases} 0 = e_2^\star \\ 0 = \frac{k_{11}}{m} e_1^\star - 2\mu g(\lambda_1^\star(t) - \lambda_{1d}(t)) \\ 0 \le \lambda_d(t) \perp w_d(t) = \begin{pmatrix} 0 & 1 \\ 0 & 0 \end{pmatrix} u_d(t) + \begin{pmatrix} 0 \\ 1 \end{pmatrix} + \begin{pmatrix} 0 & 1 \\ -1 & 0 \end{pmatrix} \lambda_d(t) + \begin{pmatrix} 0 & -1 \\ 0 & 0 \end{pmatrix} x_d(t) \ge 0 \\ 0 \le \lambda^\star(t) \perp w^\star(t) = \begin{pmatrix} k_{21} & k_{22} - 1 \\ 0 & 0 \end{pmatrix} e^\star(t) + \begin{pmatrix} g_{21} & 1 \\ -1 & 0 \end{pmatrix} \lambda^\star(t) - \begin{pmatrix} g_{21} & 0 \\ 0 & 0 \end{pmatrix} \lambda_d(t) \\ \qquad + \begin{pmatrix} 0 & 1 \\ 0 & 0 \end{pmatrix} u_d(t) \ge 0 \end{cases} \tag{68}$$

The problem in (68) is a mixed LCP with unknowns $e_1^\star$, $e_2^\star$, $\lambda_1^\star$, $\lambda_2^\star$. The equilibrium point of the error dynamics is given by $e_1^\star(t) = \frac{2m\mu g}{k_{11}}(\lambda_1^\star(t) - \lambda_{1d}(t))$. It is dependent on the complementarity variables λ_{1d} and $\lambda_1^\star$. In the above analysis, the LCP of the desired system is solved which gives the values of λ_d and x_d. Now, it is required to solve the LCP of the closed-loop system (*i.e.,* $0 \le \lambda^\star \perp w^\star \ge 0$) in order to find $\lambda^\star$ and then calculate the equilibrium point $e_1^\star$. Let us substitute $e^\star$ in terms of $\lambda^\star$ and λ_d, then the LCP to be solved is:

$$0 \le \begin{pmatrix} \lambda_1^\star(t) \\ \lambda_2^\star(t) \end{pmatrix} \perp \begin{pmatrix} w_1^\star(t) \\ w_2^\star(t) \end{pmatrix} = \begin{pmatrix} 2m\mu g\frac{k_{21}}{k_{11}} + g_{21} & 1 \\ -1 & 0 \end{pmatrix} \begin{pmatrix} \lambda_1^\star(t) \\ \lambda_2^\star(t) \end{pmatrix} + \begin{pmatrix} -2m\mu g\frac{k_{21}}{k_{11}} - g_{21} & 0 \\ 0 & 0 \end{pmatrix} \begin{pmatrix} \lambda_{1d}(t) \\ \lambda_{2d}(t) \end{pmatrix} + \begin{pmatrix} u_{2d}(t) - x_{2d}(t) \\ 1 \end{pmatrix} \ge 0 \tag{69}$$

It is important to note that the system can be at equilibrium, while the multipliers are time-varying. We can observe the new term $2m\mu g\frac{k_{21}}{k_{11}} + g_{21}$, that appears in the matrix of the multiplier $\lambda^\star(t)$ in (69). This term plays a significant role in the subsequent analysis of the equilibrium point, so let us study the sign of this term. Let Assumption 1 holds for the closed-loop system in (15), then it is necessary to ensure that the following holds:

$$-A_{cl}^\top P - PA_{cl} - \epsilon P \succeq 0 \tag{70}$$

where $P = P^\top = \begin{pmatrix} p_{11} & p_{12} \\ p_{12} & p_{22} \end{pmatrix} \succ 0$ and $\epsilon > 0$. Hence, the matrix inequality in (70) is written as:

$$\begin{pmatrix} -\frac{2k_{11}}{m}p_{12} & -p_{11} - \frac{k_{11}}{m}p_{22} - \frac{k_{12}}{m}p_{12} \\ -p_{11} - \frac{k_{11}}{m}p_{22} - \frac{k_{12}}{m}p_{12} & -2p_{12} - \frac{2k_{12}}{m}p_{22} \end{pmatrix} - \epsilon \begin{pmatrix} p_{11} & p_{12} \\ p_{12} & p_{22} \end{pmatrix} \succeq 0 \tag{71}$$

According to the equality implied by passivity, $PB_{cl} = C_{cl}^\top$ since $D_{cl} + D_{cl}^\top = 0$, we have $-2p_{12}\mu g = k_{21}$ and $-2p_{22}\mu g = k_{22} - 1$. Let us substitute the value of p_{12} in (71), then

$$-\frac{2k_{11}}{m}p_{12} - \epsilon p_{11} \geq 0 \Leftrightarrow \frac{k_{11}k_{21}}{m\mu g} - \epsilon p_{11} \geq 0$$

Given that $p_{11} > 0$, then $\frac{k_{11}k_{21}}{m\mu g}$ must be positive. This means that k_{11} and k_{21} have same signs. So, the term $2m\mu g\frac{k_{21}}{k_{11}}$ and according to Assumption 1 that imposes strict passivity on the closed-loop system, ≥ 0. Hence, the term $2m\mu g\frac{k_{21}}{k_{11}} + g_{21}$ which is multiplied by $\lambda_1^\star(t)$ is non-negative. In order to study the well-posedness of the closed-loop system's LCP in (69), let us consider different cases as above:

case 1: $\lambda_1^\star \in]0, 1[$ In this case, $w_1^\star = (2m\mu g\frac{k_{21}}{k_{11}} + g_{21})(\lambda_1^\star - \lambda_{1d}) = 0$. Hence, $\lambda_1^\star = \lambda_{1d}$. The solutions are given by: $\begin{cases} \lambda^\star = (\lambda_{1d}, 0)^\top \\ w^\star = (0, 1 - \lambda_{1d})^\top \end{cases}$.

case 2: $\lambda_1^\star = 0$ In this case, $w_1^\star = -(2m\mu g\frac{k_{21}}{k_{11}} + g_{21})\lambda_{1d} + u_{2d} - x_{2d} \geq 0$ which holds only if $u_{2d} - x_{2d} \geq 0$. If $u_{2d} - x_{2d} > 0$, then the solution of the desired LCP in (68) is:

$$\begin{cases} \lambda_d = (0, 0)^\top \\ w_d = (u_{2d} - x_{2d}, 1)^\top \end{cases}$$

If $u_{2d} - x_{2d} = 0$, then the solution is $\lambda_{1d} = 0$. Thus, in this case, $\lambda_1^\star = \lambda_{1d} = 0$. The unique solution is given by: $\begin{cases} \lambda^\star = (0, 0)^\top \\ w^\star = (u_{2d} - x_{2d}, 1)^\top \end{cases}$.

case 3: $\lambda_1^\star = 1$ In this case, $w_1^\star = (2m\mu g\frac{k_{21}}{k_{11}} + g_{21})(1 - \lambda_{1d}) + \lambda_2^\star + u_{2d} - x_{2d} = 0 \Rightarrow \lambda_2^\star = -(2m\mu g\frac{k_{21}}{k_{11}} + g_{21})(1 - \lambda_{1d}) + x_{2d} - u_{2d} \geq 0$ which holds only if $x_{2d} - u_{2d} \geq 0$. If $x_{2d} - u_{2d} > 0$, then the solution of the desired system's LCP in (68) is:

$$\begin{cases} \lambda_d = (1, x_{2d} - u_{2d})^\top \\ w_d = (0, 0)^\top \end{cases}$$

If $x_{2d} - u_{2d} = 0$, then the inequality $-(2m\mu g\frac{k_{21}}{k_{11}} + g_{21})(1 - \lambda_{1d}) \geq 0$ holds if and only if $\lambda_{1d} = 0$. So, $\lambda_1^\star = \lambda_{1d} = 1$. The solution is unique and it is given by: $\begin{cases} \lambda^\star = (1, x_{2d} - u_{2d})^\top \\ w^\star = (0, 0)^\top \end{cases}$

Therefore, in all the possible cases of $\lambda_1^\star$, it is observed that $\lambda_1^\star = \lambda_{1d}$. It is noteworthy that in all cases, we have $\lambda^\star = \lambda_d$ and $w^\star = w_d$. Given that $e_1^\star = \frac{2m\mu g}{k_{11}}(\lambda_1^\star(t) - \lambda_{1d}(t))$ and $\lambda^\star(t) = \lambda_d(t)$, then $e^\star = (e_1^\star, e_2^\star)^\top = (0,0)^\top$. This is in accordance with the fact that Proposition 2 guarantees global exponential stability (hence uniqueness of the origin of the error dynamics).

References

[1] *MOSEK ApS, MOSEK Optimizer API for Python*, 2023. https://docs.mosek.com/10.1/pythonapi.pdf.

[2] V. Acary, O. Bonnefon, M. Brémond, O. Huber, F. Pérignon, and S. Sinclair. An introduction to Siconos. Technical Report RT-0340, INRIA, 2019. https://inria.hal.science/inria-00162911v3/file/RR-0340-v3.pdf.

[3] V. Acary and B. Brogliato. *Numerical Methods for Nonsmooth Dynamical Systems: Applications in Mechanics and Electronics*, volume 35. Springer Verlag, 2008.

[4] U. Andreaus and P. Casini. Dynamics of friction oscillators excited by a moving base and/or driving force. *Journal of Sound and Vibration*, 245:685–699, 2001.

[5] B. Armstrong-Hélouvry. *Control of Machines with Friction*. Springer New York, NY, 1 edition, 1991.

[6] M. Barreau, S. Tarbouriech, and F. Gouaisbaut. Lyapunov stability analysis of a massâspring system subject to friction. *Systems and Control Letters*, 150:104910, 2021.

[7] J. Bastien, M. Schatzman, and C. Lamarque. Study of an elastoplastic model with an infinite number of internal degrees of freedom. *European Journal of Mechanics - A/Solids*, 21(2):199–222, 2002.

[8] H. H. Bauschke and P. L. Combettes. *Convex Analysis and Monotone Operator Theory in Hilbert Spaces*. Canadian Mathematical Society–Société mathématique du Canada. Springer Science+Business Media, 2011.

[9] R. Beerens, A. Bisoffi, L. Zaccarian, W. P. M. H. Heemels, H. Nijmeijer, and N. van de Wouw. Hybrid PID control for transient performance improvement of motion systems with friction. In *2018 Annual American Control Conference (ACC)*, pages 539–544, 2018.

[10] R. Beerens, H. Nijmeijer, W. P. M. H. Heemels, and N. van de Wouw. Set-point control of motion systems with uncertain set-valued stribeck friction. *IFAC-PapersOnLine*, 50(1):2965–2970, 2017. 20th IFAC World Congress.

[11] E.J. Berger. Friction modeling for dynamic system simulation. *Applied Mechanics Reviews*, 55(6):535–577, 10 2002.

[12] D. S. Bernstein. *Matrix Mathematics. Theory, Facts and Formulas*. Princeton Univ. Press, 2nd ed. edition, 2009.

[13] B. Brogliato. *Nonsmooth Mechanics. Models, Dynamics, and Control*. Communications and Control Eng. Springer Int. Pub. Switzerland, 3rd edition, 2016.

[14] B. Brogliato. Dissipative dynamical systems with set-valued feedback loops: Well-posed set-valued Lurâe dynamical systems. *IEEE Control Systems*, 42(3):93–114, 2022.

[15] B. Brogliato. Modeling, analysis and control of robotâobject nonsmooth underactuated lagrangian systems: A tutorial overview and perspectives. *Annual Reviews in Control*, 55:297–337, 2023.

[16] B. Brogliato, R. Lozano, B. Maschke, and O. Egeland. *Dissipative Systems Analysis and Control*. Communications and Control Eng. Springer Nature Switzerland AG, 3rd edition, 2020. Erratum/addendum at https://inria.hal.science/hal-03364924v3/document.

[17] B. Brogliato and A. Tanwani. Dynamical systems coupled with monotone set-valued operators: Formalisms, applications, well-posedness, and stability. *SIAM Review*, 62(1):3–129, 2020.

[18] B. Brogliato and L. Thibault. Existence and uniqueness of solutions for non-autonomous complementarity systems. *Journal of Convex Analysis*, 17(3-4):961–990, 2010.

[19] A. Cabboi, L. Marino, and A. Cicirello. A comparative study between AmontonsâCoulomb and DieterichâRuina friction laws for the cyclic response of a single degree of freedom system. *European Journal of Mechanics - A/Solids*, 96:104737, 2022.

[20] K. Camlibel. *Complementarity Methods in the Analysis of Piecewise Linear Dynamical Systems*. PhD thesis, Katholieke Universiteit Brabant, Tilburg, NL, 2001. ISBN 90 5668 079 X.

[21] M. K. Camlibel, W. P. M. H. Heemels, and J. M. Schumacher. On linear passive complementarity systems. *European Journal of Control*, 58:220–237, 2002.

[22] M. K. Camlibel, L. Iannelli, and A. Tanwani. Convergence of proximal solutions for evolution inclusions with time-dependent maximal monotone operators. *Mathematical Programming Ser. A*, 145:1017–1059, 2021.

[23] M. K. Camlibel, L. Iannelli, and F. Vasca. Passivity and complementarity. *Mathematical Programming Ser. A*, 145:531–563, 2014.

[24] M. Corless and G. Leitmann. Continuous state feedback guaranteeing uniform ultimate boundedness for uncertain dynamic systems. *IEEE Transactions on Automatic Control*, 26(5):1139–1144, 1981.

[25] R. W. Cottle, J. S. Pang, and R. E. Stone. *The Linear Complementarity Problem*. Academic Press, 1992.

[26] G. Csernák and G. Licskó. Asymmetric and chaotic responses of dry friction oscillators with different static and kinetic coefficients of friction. *Meccanica*, 56, 06 2021.

[27] G. Csernák and G. Stépán. On the periodic response of a harmonically excited dry friction oscillator. *Journal of Sound and Vibration*, 295(3):649–658, 2006.

[28] J. Das and A.K. Mallik. Control of friction driven oscillation by time-delayed state feedback. *Journal of Sound and Vibration*, 297(3):578–594, 2006.

[29] J. C. A. de Bruin, A. Doris, N. van de Wouw, W. P. M. H. Heemels, and H. Nijmeijer. Control of mechanical motion systems with non-collocation of actuation and friction: A Popov criterion approach for input-to-state stability and set-valued nonlinearities. *Automatica*, 45(2):405–415, 2009.

[30] J. P. Den Hartog. Forced vibrations vith combined Coulomb and viscous friction. *Transactions of the American Society of Mechanical Engineers*, 53(2):107–115, 1930.

[31] M. di Bernardo, C.J. Budd, A.R. Champneys, and P. Kowalczyk. *Piecewise-smooth Dynamical Systems. Theory and Applications*. Number 163 in Applied Mathematical Sciences. Springer-Verlag, London, 2008.

[32] B. A. Erickson, B. Birnir, and D. Lavallee. Periodicity, chaos and localization in a Burridge-Knopoff model of an earthquake with rate-and-state friction. *Geophysical Journal International*, 187:178 – 198, 08 2011.

[33] F. Facchinei and J. S. Pang. *Finite-Dimensional Variational Inequalities and Complementarity Problems, Volume I*. Operations Research and Financial Engineering. Springer, New York, 2003.

[34] B. C. Gegg, A. C.J. Luo, and S. C. Suh. Grazing bifurcations of a harmonically excited oscillator moving on a time-varying translation belt. *Nonlinear Analysis: Real World Applications*, 9(5):2156–2174, 2008.

[35] S. Greenhalgh, V. Acary, and B. Brogliato. On preserving dissipativity properties of linear complementarity dynamical systems with the theta-method. *Numerische Mathematik*, 125(4):601–637, 2013.

[36] M. A. Heckl and I.D. Abrahams. Active control of friction-driven oscillations. *Journal of Sound and Vibration*, 193(1):416–426, 1996.

[37] W. P. M. H. Heemels, V. Sessa, F. Vasca, and M. K. Camlibel. Computation of periodic solutions in maximal monotone dynamical systems with guaranteed consistency. *Nonlinear Analysis: Hybrid Systems*, 24:100–114, 2017.

[38] N. Hinrichs, M. Oestreich, and K. Popp. On the modelling of friction oscillators. *Journal of Sound and Vibration*, 216(3):435–459, 1998.

[39] R. A. Horn and C. R. Johnson. *Matrix Analysis*. Cambridge University Press, 2nd edition, 2013.

[40] H.K. Khalil. *Nonlinear Systems*. Prentice Hall, Upper Saddle River, NJ, 3rd edition, 2002.

[41] R. Kikuuwe, S. Yasukouchi, H. Fujimoto, and M. Yamamoto. Proxy-based sliding mode control: A safer extension of PID position control. *IEEE Transactions on Robotics*, 26(4):670–683, 2010.

[42] Y. B. Kim and S. T. Noah. Stability and bifurcation analysis of oscillators with piecewise-linear characteristics: A general approach. *Journal of Applied Mechanics*, 58(2):545–553, 06 1991.

[43] M. Kunze. *Non-smooth Dynamical Systems*. Number 1744 in Lecture Notes in Mathematics. Springer-Verlag, Berlin Heidelberg, 2000.

[44] M. Legrand and C. Pierre. A compact, equality-based weighted residual formulation for periodic solutions of systems undergoing frictional occurrences. *Journal of Structural Dynamics*, 2:144–170, 2024.

[45] R. I. Leine and H. Nijmeijer. *Dynamics and Bifurcations of Non-Smooth Mechanical Systems*. Number 18 in Lecture Notes in Applied and Computational Mechanics. Springer-Verlag, Berlin Heidelberg, 2004.

[46] R. I. Leine and D. H. van Campen. Discontinuous bifurcations of periodic solutions. *Mathematical and Computer Modelling*, 36:259–273, 2002.

[47] R. I. Leine, D. H. van Campen, A. de Kraker, and L. van den Steen. Stick-slip vibrations induced by alternate friction models. *Nonlinear Dynamics*, 16(1):41–54, 1998.

[48] R. I. Leine, D. H. van Campen, and B. Vrande. Bifurcations in nonlinear discontinuous systems. *Nonlinear Dynamics*, 23:105–164, 2000.

[49] Y. Li and Z.C Feng. Bifurcation and chaos in friction-induced vibration. *Communications in Nonlinear Science and Numerical Simulation*, 9(6):633–647, 2004.

[50] Z. Li, H. Ouyang, Y. Gu, S. Martelli, S. Yang, H. Wei, W. Wang, and R.H. Wei. Non-stationary friction-induced vibration with multiple contact points. *Nonlinear Dynamics*, 111:9889–9917, 2023.

[51] Z. Li, Q. Wang, and H.-P. Gao. Control of friction oscillator by Lyapunov redesign based on delayed state feedback. *Acta Mechanica Sinica*, 25:257–264, 2009.

[52] C. S. Liu and W. T. Chang. Frictional behaviour of a belt-driven and peridiocally excited oscillators. *Journal of Sound and Vibration*, 258(2):247–268, 2002.

[53] Y. F. Liu, J. Li, Z. M. Zhang, X. H. Hu, and W. J. Zhang. Experimental comparison of five friction models on the same test-bed of the micro stick-slip motion system. *Mechanical Sciences*, 6:15–28, 2015.

[54] A. C. J. Luo and B. C. Gegg. Periodic motions in a periodically forced oscillator moving on an oscillating belt with dry friction. *Journal of Computational and Nonlinear Dynamics*, 1(3):212–220, 03 2006.

[55] A.C. J. Luo and M.T. Patel. Bifurcation and stability of periodic motions in a periodically forced oscillator with multiple discontinuities. *Journal of Computational and Nonlinear Dynamics*, 4(1):011011, 12 2008.

[56] C. Makkar, G. Hu, W. G. Sawyer, and W. E. Dixon. Lyapunov-based tracking control in the presence of uncertain nonlinear parameterizable friction. *IEEE Transactions on Automatic Control*, 52(10):1988–1994, 2007.

[57] N. Mallon, N. van de Wouw, D. Putra, and H. Nijmeijer. Friction compensation in a controlled one-link robot using a reduced-order observer. *IEEE Transactions on Control Systems Technology*, 14(2):374–383, 2006.

[58] L. Marino and A. Cicirello. Experimental investigation of a single-degree-of-freedom system with Coulomb friction. *Nonlinear Dynamics*, 99:1781–1799, 2020.

[59] K. Mehran, B. Zahawi, D. Giaouris, and J. Wang. Stability analysis of slidingâgrazing phenomenon in dry-friction oscillator using Takagi-Sugeno fuzzy approach. *Journal of Computational and Nonlinear Dynamics*, 10(6):061010, 11 2015.

[60] M. Oestreich, N. Hinrichs, and K. Popp. Bifurcation and stability analysis for a non-smooth friction oscillator. *Archive of Applied Mechanics*, 66(5):301–314, 1996.

[61] E. Panteley, R. Ortega, and M. Gäfvert. An adaptive friction compensator for global tracking in robot manipulators. *Systems & Control Letters*, 33(5):307–313, 1998.

[62] Q. H. Pham and B. Brogliato. Correction to "Analysis of the implicit Euler time-discretization of a class of descriptor-variable linear cone complementarity systems", J. Convex Analysis 29/2 (2022) 481–517. *Journal of Convex Analysis*, 31(3):1035–1037, 2024.

[63] K. Popp and P. Stelter. Stick-slip vibrations and chaos. *Philosophical Transactions: Physical Sciences and Engineering*, 332(1624):89–105, 1990.

[64] D. Putra, H. Nijmeijer, and N. van de Wouw. Analysis of undercompensation and overcompensation of friction in 1-dof mechanical systems. *Automatica*, 43(8):1387–1394, 2007.

[65] R. T. Rockafellar. *Convex Analysis*. Princeton University Press, New Jersey, 1970.

[66] R. T. Rockafellar and R. J. B. Wets. *Variational Analysis*, volume 317 of *Grundlehren der mathematischen Wissenschaften*. Springer Verlag, Berlin Heidelberg, 2009. Corrected Third Printing.

[67] C. Scherer and S. Weiland. *Linear Matrix Inequalities in Control*. 2015. https://www.imng.uni-stuttgart.de/mst/files/LectureNotes.pdf.

[68] M. Schuderer, G. Rill, T. Schaeffer, and C. Schulz. Friction modeling from a practical point of view. *Multibody System Dynamics*, pages 1–18, 2024.

[69] S. W. Shaw. On the dynamic response of a system with dry friction. *Journal of Sound and Vibration*, 108:305–325, 1986.

[70] E.D. Sontag. *Mathematical Control Theory: Deterministic Finite Dimensional Systems*. Texts in Applied Mathematics. Springer, New York, 2013.

[71] S. Southward, C. Radcliffe, and C. MacCluer. Robust nonlinear stick-slip friction compensation. *Journal of Dynamic Systems Measurement and Control*, 113, 12 1991.

[72] A. Taware, G. Tao, N. Pradhan, and C. Teolis. Friction compensation for a sandwich dynamic system. *Automatica*, 39(3):481–488, 2003.

[73] J.J. Thomsen. Using fast vibrations to quench friction-induced oscillations. *Journal of Sound and Vibration*, 228(5):1079–1102, 1999.

[74] J.J. Thomsen and A. Fidlin. Analytical approximations for stick-slip vibration amplitudes. *International Journal of Non-Linear Mechanics*, 38:389–403, 04 2003.

[75] N. van de Wouw and R. I. Leine. Robust impulsive control of motion systems with uncertain friction. *International Journal of Robust and Nonlinear Control*, 22(4):369–397, 2011.

[76] P. Vigué, C. Vergez, S. Karkar, and B. Cochelin. Regularized friction and continuation: Comparison with Coulomb's law. *Journal of Sound and Vibration*, 389:350–363, 2017.

[77] A. Younes, F. Miranda-Villatoro, and B. Brogliato. Trajectory tracking in linear complementarity systems with and without state jumps: A passivity approach. *Nonlinear Analysis: Hybrid Systems*, 54:101520, 2024.